SLOWKIN: A Simplified Model for the Simulation of Transients in a SLOWPOKE–2 Reactor

DANIEL ROZON,
SIAMAK KAVEH

Institut de génie nucléaire
École Polytechnique de Montréal
P. O. Box 6079, Succursale "Centre-ville"
Montréal, Québec H3C 3A7

Report IGE-219 (rev.1)
August 1997

CONTENTS

List of Tables

List of Figures

1. INTRODUCTION

This report describes the model used to analyse reactor transients in the SLOWPOKE–2 reactor at École Polytechnique. The model is specifically intended to simulate reactor transients caused by control rod displacements during commissionning of the new LEU core to be installed in the SLOWPOKE–2 reactor in 1997, in replacement of the original HEU core. A simplified treatment is justified since our objective is mainly to provide a physical interpretation for any difference observed in the transient behaviour of the new core, as opposed to the current HEU core.

The SLOWPOKE–2 reactor is a small pool-type reactor, illustrated in Fig. 1. The current HEU core is composed of 296 aluminium/uranium alloy fuel pins, disposed on a hexagonal lattice and containing highly enriched uranium (93%). The core, through which flows the light-water coolant, forms a thightly coupled undermoderated lattice. The core is surrounded by the berylium reflector, moderating the leaking neutrons and providing a high thermal neutron flux in the irridiation sites located in the metallic reflector.

The single control rod is inserted in the center of the lattice. It moves up and down to regulate the flux level at the site of the control detector, also located in the berylium reflector. During commissionning, the number of pins in the core is adjusted to provide limited excess reactivity in the fuel (between 3.4 and 4.0 mk), with sufficient shutdown margin. For the current HEU core, the control rod worth is approximately 5.4 mk, with a maximum insertion 5.7 cm above the bottom reflector.

A specific feature of the SLOWPOKE–2 reactor is the inherent self-limiting feedback which allows fully automatic (unsupervised) operation and justifies the absence of an emergency shutdown system: because the lattice is undermoderated, any reduction of coolant density will have a negative reactivity effect. This is the dominant effect of a rise in moderator water temperature as a result of an increase in reactor power.

Other temperature reactivity effects are also present, to a lesser extent. Fuel temperature effects are negligeable in HEU, but can become important in LEU because of the Doppler reactivity associated with a much larger U-238 content, coupled with the lower conductivity and higher temperature of the ceramic fuel. The water in the reactor container flowing outside of the metallic berylium reflector constitutes an outer reflector for leaking neutrons. Temperature changes in this region can thus have a (smaller) positive reactivity effect. The temperature of the beryllium reflector could also affect slightly the reactivity balance.

Finally, for fast transients, the fuel sheath temperature may exceed the water saturation temperature so that onset of nucleate boiling (ONB) will occur. Because of a highly negative void coefficient, significant antireactivity can be introduced beyond ONB. The SLOWKIN model must therefore be able to predict the small void fractions following ONB since void formation may very well become the dominant negative feedback beyond a certain power level.

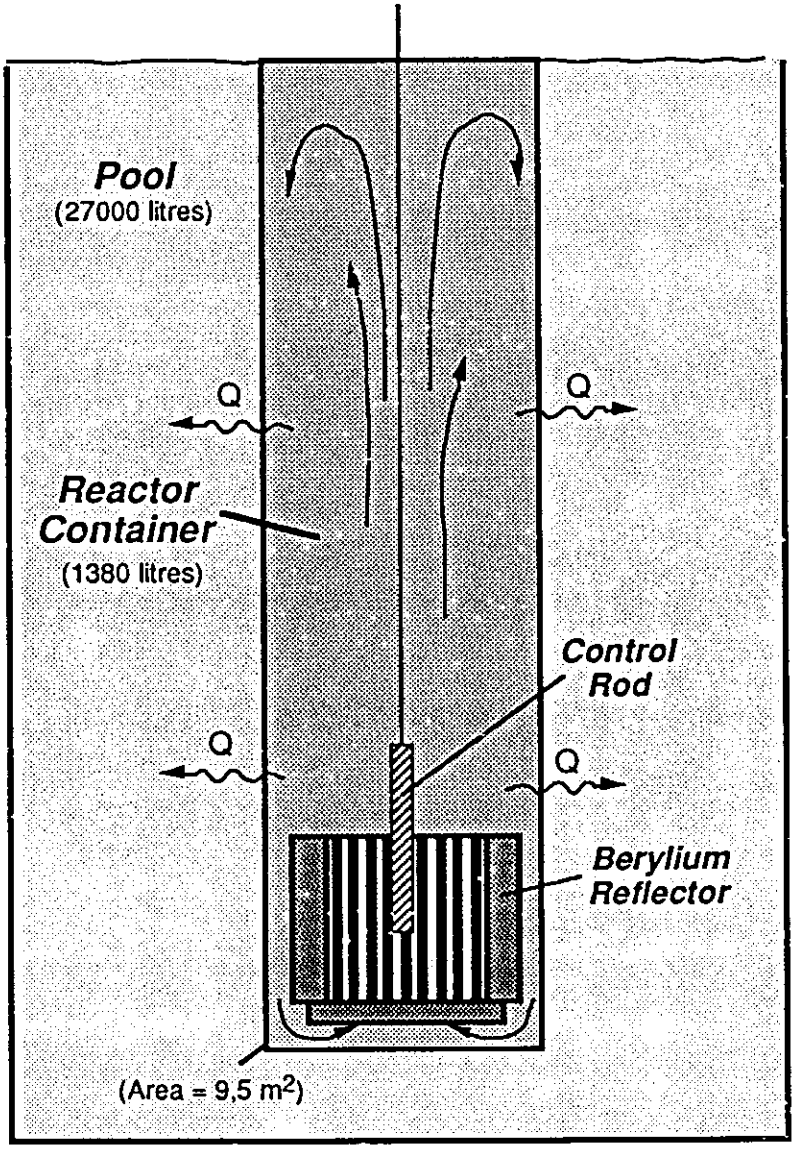

Figure 1: The SLOWPOKE-2 Rcactor

2. THE SLOWKIN MODEL

The SLOWKIN model uses point kinetics to predict neutron power with time. Conservation of mass and energy is applied to write the lumped parameter equations for the temperature within the regions of interest. The core region is subdivided into an arbitrary number of axial planes along which the radial heat transfer in an average fuel pin will be considered.

A simple one-dimensional model will be used to calculate the steady state natural circulation of water through the core. A sampled first-order filter will introduce a simple time-constant delay to represent the inertial effects. All water properties are calculated at constant pressure, the hydrostatic pressure at mid-core depth in the pool (1.435 *bar*). This major simplication allows us to simulate a transient without solving the thermalhydraulics equations for natural circulation.

The resulting set of ODE's are integrated in SLOWKIN using an ODE solver found in the litterature.[1] The reactor physics codes DRAGON/DONJON developped at École Polytechnique can be used to provide the necessary reactivity coefficients.[2, 3, 4]

Three types of simulations can be carried out with SLOWKIN:

1. The constant power operation, where the reactor is at steady-state (critical) but the temperature varies as a function of time, causing observed control rod movements. Long term (hours) simulations can predict the operating margin in the absence of cooling in the pool;

2. Automatic control rod movements can cause power variations. A steady state power level must first be given, with the reactor critical or subcritical. A setpoint power is then specified, and the control rod is displaced until the desired power is acheived. These movements thus simulate a start-up or a power manoeuvre. The reactivity excursions planned for the Commissionning [5] will be simulated by demanding an arbitrarily high power starting from zero power;

3. The control rod is held at a fixed position, which can be different than the initial position. Also, an arbitrary reactivity echelon or ramp can be introduced.

2.1 Point Kinetics

The neutronic analysis of the SLOWPOKE–2 reactor starts with a detailed representation of the reactor domain, using a chain of deterministic codes. Our model starts with a full-core 2D cluster in DRAGON to generate a detailled spectrum in transport theory. The nuclear cross sections are then homogenized over material regions of interest and condensed to a few energy groups for subsequent 3D diffusion calculations in DONJON. Our initial study shows that 6 energy groups are adequate for full-core diffusion calculations in the SLOWPOKE reactor.[6] The TRIVAC–3 module of DONJON solves the multigroup diffusion equation using an hexagonal mesh where each fuel pin is represented explicitly. As shown in Figs. 2 and 3, the reactor domain for the diffusion calculations contains over

55000 points and extends radially 5.6 cm into the pool water where the neutron flux is assumed to vanish.

We can write generally for the diffusion calculation:

$$(\mathbf{M} - \lambda \mathbf{F})\,\phi = 0\,, \tag{1}$$

where **M** is the neutron elimination operator (absorption, scattering and leakage) and **F** is the production operator (fission + delayed neutrons). λ is the eigenvalue, equal to $\frac{1}{k_{\text{eff}}}$.

The point kinetics equations are obtained from the time-dependent diffusion equation by introducing the following flux factorisation:

$$\phi(\vec{r}, E, t) = p(t)\psi(\vec{r}, E)\,, \tag{2}$$

where $p(t)$ is the time-dependent amplitude and ψ is the fixed flux shape, usually corresponding to the initial steady-state conditions. The amplitude is arbitrarily normalized to one at the beginning of a transient:

$$p(0) = p_o = 1.0\,. \tag{3}$$

The point kinetics equations can be written:[7]

$$\Lambda \frac{dp}{dt} = [\rho(t) - \beta]\, p(t) + \sum_{k=1}^{K} \lambda_k \zeta_k(t) + s(t) \tag{4}$$

$$\frac{d\zeta_k}{dt} = -\lambda_k \zeta_k(t) + \beta_k\, p(t) \tag{5}$$

where $\zeta_k(t)$ is the weighted precursor concentration in delayed group k. $s(t)$ is the weighted external source (if present). The steady-state initial conditions are either for a critical reactor, in which case both the source $s(t)$ and the dynamic reactivity $\rho(t)$ are initially zero, or for a subcritical reactor, where the initial conditions are a constant (negative) reactivity $\rho(0) = \rho_o$, with the source strength equal to:

$$s(0) = -\rho_o p_o\,. \tag{6}$$

We see that the source strength is implicitly chosen when specifying the initial neutron power level in a subcritical reactor.

An adiabatic approximation will be used for the dynamic reactivity, i.e. it will be obtained from the static reactivity provided by the DONJON diffusion calculations (the eigenvalue associated with a particular steady state of the reactor):

$$\rho = 1.0 - \lambda \tag{7}$$

$$= \frac{\langle \phi_o^*, (\mathbf{F} - \mathbf{M})\phi \rangle}{\langle \phi_o^*, \mathbf{F}\phi \rangle}\,. \tag{8}$$

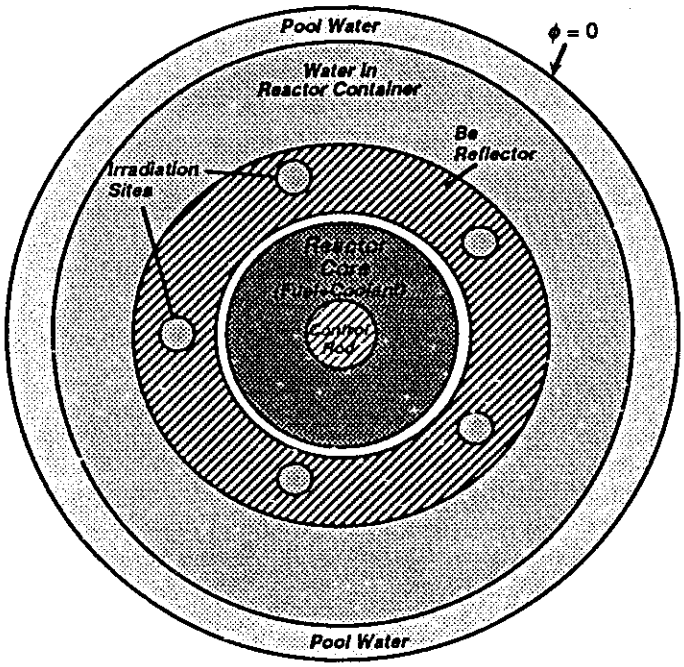

Figure 2: The Reactor Domain for Diffusion Calculations in DONJON (Top View)

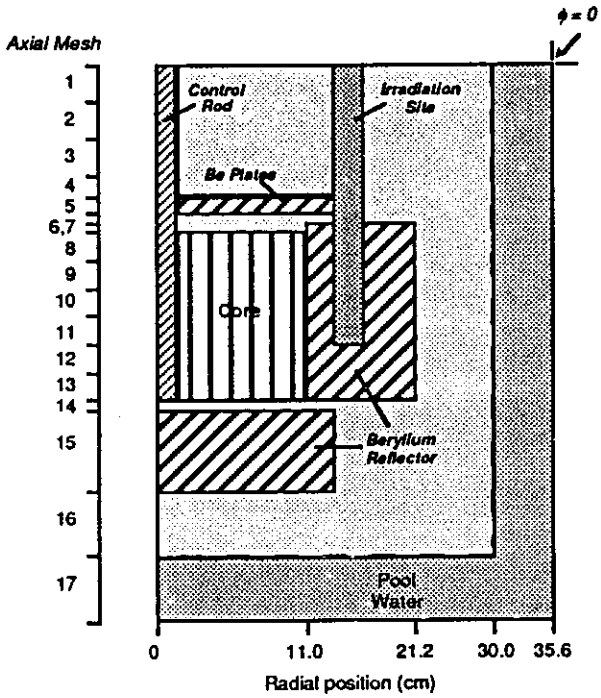

Figure 3: The Reactor Domain for Diffusion Calculations in DONJON (Elevation)

where the bracket notation $< , >$ has been introduced to signify integration over phase-space. We note in Eq. (8) that ϕ is the *perturbed* flux (at time t) and that M and F are the perturbed operators. ϕ_o^* is the adjoint flux, solution to the adjoint equations in the initial steady-state. These can also be calculated in the TRIVAC diffusion modules of DONJON. We have:

$$(\mathbf{M}_o^* - \lambda_o \mathbf{F}_o^*)\, \phi_o^* = 0 \tag{9}$$

For dynamic reactivity, we could write:

$$\rho(t) = \rho\left(0^+\right) + \frac{\langle \phi_o^*, [\delta\mathbf{M}(t) - \lambda_o \delta\mathbf{F}(t)]\, \phi \rangle}{\langle \phi_o^*, \mathbf{F}\phi \rangle} \,. \tag{10}$$

where operators $\delta\mathbf{M}(t)$ and $\delta\mathbf{F}(t)$ contain the *variations* in macroscopic cross sections after time $t = 0^+$, e.g. the variations introduced by the temperature changes during the transient.

The effective delayed neutron fraction can be written:[7]

$$\beta_k(t) = \frac{\langle \phi_o^*, \mathbf{F}_{dk}\phi \rangle}{\langle \phi_o^*, \mathbf{F}\phi \rangle} \,, \tag{11}$$

which can be evaluated for the reference core and considered constant. In SLOWKIN, we have used the isotopic delayed group constants for U-235 given in Table 2. A spectral correction is applied to reflect the importance of the delayed neutron emission spectrum within the lattice. Since both LEU and HEU are undermoderated lattices, and because the delayed neutron spectrum is softer than the prompt fission neutron emission spectrum, this correction tends to *increase* the effective delayed neutron fraction. The following values of β have been used, taken from the Safety Report:[8]

Table 1: Effective Delayed Neutron Fraction

	β	*Spectral Correction*
HEU	0.83110 %	1.190
LEU	0.81923 %	1.173

We note finally that a small number of delayed photoneutrons can be produced in the berylium reflector. As a first approximation and in order to determine the influence of photoneutrons on the transient behaviour of the reactor, we introduced 9 additionnal delayed neutron groups, using the photoneutron data for CANDU reactors,[9] but limiting the total contribution of photoneutrons to only 1% of β. For a fast transient in HEU (5 mk), it was found that the presence of these photoneutrons reduces the prompt peak by approximately 5%, but it has very little effect on the value of the delayed peak (reduction of 0.2%). Since we are mostly interested in the latter (for comparison with commissionning measurements), the use of this option in SLOWKIN is not considered essential.

Table 2: Delayed Neutron Group Properties for U-235

Group	λ_k (s^{-1})	β_k (%)
1	0.0129	0.0251
2	0.0311	0.1545
3	0.1340	0.1476
4	0.3310	0.2663
5	1.2600	0.0756
6	3.2100	0.0293
total	-	0.6984

The mean generation time is given by:

$$\Lambda(t) = \frac{\left\langle \phi_o^*, \frac{1}{v}\phi \right\rangle}{\langle \phi_o^*, \mathbf{F}\phi \rangle} , \tag{12}$$

Our preliminary calculations indicate that for the transients considered with SLOWKIN (usually, $\rho \leq \beta/2.$), results are relatively insensitive to the value of Λ.[10] In fact, we found that the Prompt Jump approximation ($\Lambda = 0$) gives a good estimate of the delayed peak power. In SLOWKIN, there is an option to use, instead of Eq. 4:

$$p(t) = \frac{\sum_{k=1}^{K} \lambda_k \zeta_k(t)}{\beta - \rho(t)} \tag{13}$$

The time-dependent solution to Eq. 4 is proportionnal to the total fission rate, and therefore $p(t)$ is proportionnal to the *total instantaneous fission power* in the reactor. Fission energy is not deposited uniformily in the reactor. Although most of the instantaneous fission power is deposited in the fuel, a fraction of nearly 6% appears in the moderator and in the reflector. Volumetric heat generation responsible for temperature changes in the reactor domain is proportionnal to $P(t)$, the *instantaneous thermal power*. $P(t)$ contains the instantaneous fission power, as well as a 7% delayed component associated with the decay power of the fission products.

We will calculate $P(t)$ as:

$$P(t) = P_o \left[(1 - \kappa_{pf}) p(t) + \sum_{i=1}^{3} \omega_i(t) \right] \tag{14}$$

$$\frac{d\omega_i}{dt} = -\lambda_i^{pf} \omega_i(t) + \kappa_i^{pf}\, p(t) \quad , \tag{15}$$

where $\kappa_{pf} = \sum_{i=1}^{3} \kappa_i^{pf} \approx 0,068$. The 3-group yields and decay constants the fission product decay heat are taken from the code SOPHT.[11]

2.2 Reactivity Coefficients

The rate of change of $p(t)$ in Eq. 4 is particularily sensitive to the current value of dynamic reactivity $\rho(t)$. Instead of recalculating $\rho(t)$ with the inner products indicated in Eq. (10), *reactivity coefficients will be calculated from differences between eigenvalues from diffusion calculations for different states (e.g. change in temperature in a material region).* This approach avoids the importance weighting in Eq. (10), and yet accounts for the steady state (or adiabatic) flux shape variations induced by the perturbations.

In SLOWKIN, reactivity will be considered a function of a number of global parameters:

$$\rho(t) = \rho_o + \rho_{cont}(t) + \rho_{temp}(t) + \rho_{void}(t) + \rho_{xenon}(t) \tag{16}$$

where ρ_o is the initial shutdown reactivity. The time dependent components are as follows:

2.2.1 Reactivity Control (ρ_{cont})

A simplified control rod model is provided in SLOWKIN. Although detailled reactivity profiles have been calculated for the control rod as a function of position,[6, 13] a simplified linear model is currently used in SLOWKIN. The total reactivity worth of the rod (ρ_b) depends on the lattice considered (HEU vs. LEU). It is also sensitive to the thickness of the berylium plates in the upper shim tray, as shown in Table 3.[13] We noted that the control rod reactivity worth in LEU is increased to 6.1 mk when full insertion is extended down to 1.6 cm from the bottom reflector.[6]

Table 3: Control Rod Worth in SLOWPOKE-2 (100%=5.7 cm)

Upper Be Plates	0 cm	1.341 cm	3.643 cm
$\rho_b^{(HEU)}$	5.187	5.235	5.415
$\rho_b^{(LEU)}$	4.488	4.447	4.716

We will assume control reactivity to be a simple function of the control rod position, $z_b(t)$ in % :

$$\rho_{cont}(t) = \rho_b[z_b(t) - z_o]/100. \tag{17}$$

where ρ_b is the rod worth calculated with the diffusion code.

z_o is the *critical rod position at zero power.* This quantity is arbitrary, but it reflects both the excess reactivity of the fuel (function of fuel burnup) and the shutdown control margin, the sum being equal to the rod worth. We note that for simulating the reactivity excursions planned during the commissionning, where the control rod is removed from the subcritical reactor, the value of z_o is adjusted to yield the desired maximum reactivity insertion.

The control rod position is determined either manually (given at input), or it is evaluated automatically. In this case, the rod displacement at half-speed or full-speed over a time step is calculated according to the sign and amplitude of the power error at the beginning of the time step. A maximum speed of 5 *cm/s* is assumed, corresponding to the current travel time of 20 *s* for a full insertion.

2.2.2 Temperature Feedback (ρ_{temp})

All temperature feedback effects are expressed relative to the same uniform reference temperature, T_o = 20°C. The temperature feedback will be function of the following average temperatures:

$T_1(t)$ The average fuel temperature in the core at time t;

$T_2(t)$ The average temperature of the water flowing through the core (coolant/moderator) at time t;

$T_3(t)$ The average temperature of the metallic berylium reflector at time t;

$T_4(t)$ The average temperature of the water reflector (water located outside of the berylium reflector flowing in the downcomer into the lower container) at time t.

In regions 2 and 4, *single phase water density variations with temperature (at a pressure of 1.4 bar) are included in the reactivity coefficients.* Temperature reactivity effects have been studied in detail in transport and diffusion theory with DRAGON/DONJON.[6, 12, 13] The following observations have been made:

- DRAGON calculations were based on three different microscopic cross section libraries: Winfrith, ENDF-B5 and ENDF-B6. Calculated reactivities in DONJON based on these different sets of cross sections were all very close, with ENDF-B5 properties marginally better in comparison with measured uniform temperature effects in SLOWPOKE-2 reactors;

- The seperate temperature effects for the 4 domains (fuel, coolant, berylium and water) were calculated in DONJON.[13] The range of temperature was 10-80°C for water (with corresponding liquid density changes), and 10 to 300°C for the fuel. Reactivity coefficients were found to be additive in the range of interest: in LEU for example, a change of 100°C in fuel temperature changes the coolant temperature *coefficient* by less than 1 %;

- Fuel temperature effects are negligeable in HEU, as expected. For LEU fuel, containing 80 % U-238, the negative (Doppler) coefficient is significant because of the much larger fuel temperature variation in the ceramic fuel;

- The most important *negative* effect is due to the moderator/coolant temperature changes. Accompanying liquid density variations account for the majority of the reactivity effect. The effect is strongly negative since the core region is undermoderated. We found that the nonlinear variation of reactivity is well represented by a *quadratic* in the range 20-80°C;

- The container water has a *positive* reactivity effect, because it lies in a fully thermalized neutron spectrum where reducing the water density reduces neutron absorption.

- The temperature of the water in the immediate vicinity of the core is not uniform. The water flowing in the downcomer is relatively cold (T_4). It is a mixture of the cold upper container water (T_5) and the warm outlet coolant ($T_{2,M}$). The degree of mixing determines the core inlet temperature ($T_{2,1} \approx T_4$). The water immediately above the core in the upper shim tray is relatively cold and is assumed equal to the upper container water temperature T_5. The reflector water temperature coefficient was calculated by varying uniformly the temperature in the lower container below the level of the outlet orifice.

- Finally, the berylium reflector contains impurities which introduce an uncertainty in k_{eff} of $\approx 5\ mk$. These impurities do not significantly influence the temperature reactivity effect associated with the metallic berylium reflector.[12] As noted in Figures 5 and 6, the reactivity effect of the berylium is also positive, but is much smaller than the positive effect of the water surrounding the core.

The temperature feedback component in SLOWKIN will therefore be written:

$$\rho_{temp}(t) = a_1\Delta T_1(t) + a_{21}\Delta T_2(t) + a_{22}\Delta T_2(t)^2 + a_3\Delta T_3(t) + a_4\Delta T_4(t) \qquad (18)$$

where $\Delta T_k(t) = T_k(t) - T_o$.

The separate temperature reactivity effects are illustrated in Figures 4 and 5. DONJON calculations show that the presence of the control rod has little influence on the moderator temperature coefficient.

Table 4: Reactivity Coefficients Calculated with DRAGON/DONJON[13]

case	a_1	a_{21}	a_{22}	a_3	a_4
HEU (1987 plates/no rod)	0.000917	-0.123875	-0.0015769	0.008178	0.042226
LEU (no plates/no rod)	-0.010165	-0.042183	-0.0015645	0.002250	0.039628
LEU (no plates/rod 79 %)	-0.010165	-0.044952	-0.0016096	0.002254	0.038912

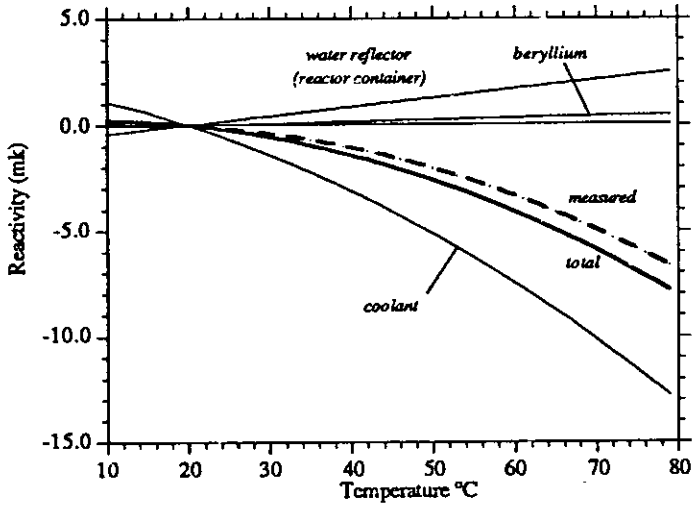

Figure 4: DRAGON/DONJON Temperature Reactivity for HEU (1987 plates-rod OUT)

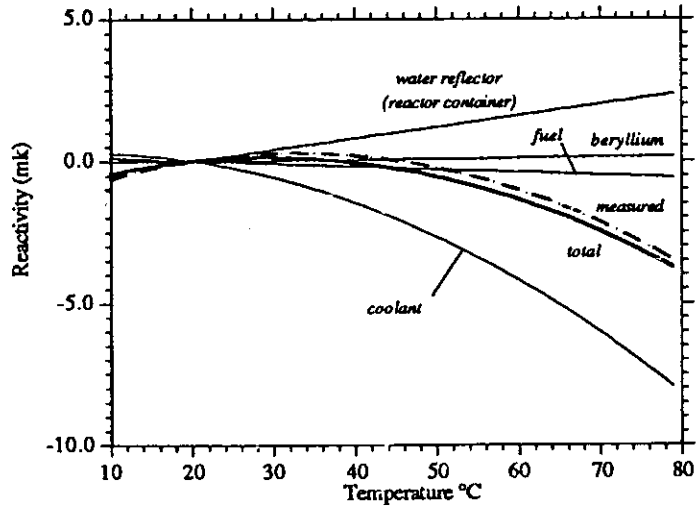

Figure 5: DRAGON/DONJON Temperature Reactivity for LEU (no plates-rod OUT)

2.2.3 Void Feedback (ρ_{void})

When power is raised in the reactor, there is a possibility that the fuel sheath temperature will exceed the saturation temperature of the water in the core. From that point on, void formation occurs through subcooled nucleate boiling. Although the volume of water displaced by steam bubbles is small, the negative reactivity introduced can be quite significant. Nucleate boiling occurs on the heating surfaces so we therefore expect void to occur near the fuel surface.

Void effects in the SLOWPOKE lattice were studied with DRAGON.[12] It was found that the void reactivity effect is mostly a function of the *average* water density, since a uniform density reduction produces nearly the same reactivity change as void located near the fuel pins. The reactivity effect is mostly due to the *displacement* of the water from the undermoderated lattice. [1]

On the other hand, water flows up through the core by natural circulation and void is likely to first appear near the outlet of the core. With DONJON diffusion calculations, we found in both HEU and LEU cores that void generation in the top (outlet) end of the core is more effective than a uniform density reduction.[13] It is seen in Table 4 that when the same quantity of void is introduced non-uniformily (2% in the top half vs.1% uniform reduction), *the reactivity effect is 26 % higher in HEU and 29 % higher in LEU.*

Table 5: DRAGON/DONJON Void Reactivity (mk) in SLOWPOKE-2

Moderator Density Reduction	HEU	LEU
1% (top half)	-2.515	-2.390
1% (total)	-3.956	-3.616
2% (top half)	-4.997	-4.656
2% (total)	-7.995	-7.218

The instantaneous distribution of void will be calculated in SLOWKIN, as described in the following sections. It is the *core-average* void fraction, $\alpha(t)$, which is used for determining feedback. However a correction will be introduced to account for the axial distribution of void (axial offset, f). To do this, the average void in the bottom half (α_1) and in the top half (α_2) will be calculated. We will determine an effective void coefficient at time t by interpolating between values in Table 5, according to:

$$\rho_{void}(t) = [b_1 \cdot f(t) + b_2 \cdot (1. - f(t))]\alpha(t) \times 100. \tag{19}$$

where the coefficients b_1 and b_2 are given in Table 6 (in $mk/\%$). The axial offset is simply $f = min\{1.0, \alpha_1/\alpha_2\}$.

[1] As a result, displacement of water by the introduction of an aluminium rod will have the nearly the same reactivity effect, and can be used for a substitution experiment to measure the void coefficient. Such a measurement is planned during commissionning of the new core at École Polytechnique.

Table 6: Void Reactivity coefficients for SLOWPOKE–2 (in $mk/\%$ void)

core	b_1	b_2
HEU	-3.956	-4.997
LEU	-3.616	-4.656

2.2.4 Xenon Feedback (ρ_{xenon})

For long-term transients, xenon build-up in the fuel can introduce a small amount of negative reactivity (≈ 0.5 mk in 10 hours). The following analytical model has been used in SLOWKIN:[7]

$$\rho_{xenon}(t) = -1.55 \times 10^{-18} N_X(t) \tag{20}$$

where the xenon concentration N_X is given by:

$$N_X(t+\Delta t) = A_1 + A_2 e^{-\lambda_I \Delta t} - (A_1 + A_2) e^{-(\lambda_X + \sigma_X \phi)\Delta t} \tag{21}$$

The constants A_1 and A_2 are functions of the iodine and xenon concentration as well as the flux level ϕ in the fuel at the beginning of the time step. We have assumed that:

$$\phi(t) = 0.7 \times 10^{12} (P_o/20) \cdot p(t) \tag{22}$$

where P_o is the reactor power at $t = 0$.

2.3 The Temperature Equations

We will now write the heat balance equations governing the temperature field in the reactor, illustrated in Figure 6. The following assumptions are made:

- Temperature is uniform within each control volume;
- A fraction $f_{rc} \approx 0.95$ of the thermal power $P(t)$ is deposited directly in the fuel. Half of the remainder ($\frac{1.-f_{rc}}{2}$) is deposited in the moderator/coolant, the rest is deposited in the berylium and water reflectors ($\frac{1.-f_{rc}}{4}$ each);
- 100% full power is defined for an absolute flux of 10^{12} $n\nu$ at the flux detector site. Because of the different flux shapes, this value is different for HEU and LEU. We found with DRAGON/DONJON that $P_o^{(LEU)}/P_o^{(HEU)} = 1.0587$.
- A natural circulation flow rate $W(t)$ is assumed through the core at time t. The value of W is related to the power delivered to the coolant (see section 2.3.7);

- Part of the water coming out of the outlet orifice is recirculated directly through the downcomer, rising the inlet temperature more rapidly. The recirculation fraction (fraction of the outlet flow not mixing with the upper container, f_{rec}) is a function of the total flow rate $W(t)$;

- The core (fuel+moderator/coolant) is subdivided into M axial regions of equal volume. Heat is transfered latterally between the fuel and coolant volumes, and between the coolant and the berylium reflector;

- Volumetric heat generation in the fuel is *not uniform*. A fixed axial power profile is assumed in the fuel. This profile was obtained from the DONJON diffusion calculations and corresponds to the steady-state axial distribution of power (averaged over each plane). If $f_{\phi m}$ is the fraction of power produced at elevation m, then the *fuel linear heat rate* q_m is simply:

$$q_m(t) = \frac{f_{rc} f_{\phi m}}{N_c H_m} \cdot P(t) \tag{23}$$

  where N_c is the number of fuel pins in the core and $H_m = H/M$ is the length of the fuel section. The linear heat rate distribution at full power is illustrated in Figure 7. *Because of the fewer fuel pins, we see that the linear heat rate is significantly higher in LEU*;

- Only radial thermal conduction is considered in the fuel pins: axial conduction is neglected;

- All water properties were evaluated for single phase liquid water at a constant pressure of 1.435 *bar*.[14]

2.3.1 Fuel (T_1)

Let us consider the temperature $T_{1,m}$ at elevation m in an average fuel pin . At steady-state, the temperature at the center of the fuel pin is given by the famous *conductivity integral*:

$$\int_{T_{sm}}^{T_{om}} k_f(\theta)\, d\theta = \frac{q_m}{4\pi} \tag{24}$$

where q_m is the local linear heat rate and the integral is carried out from the surface to the center of the fuel pin.

Let us assume that the *average* conductivity is given by:

$$\bar{k}_{fm} = k_f(T_{1,m}) \tag{25}$$

where $T_{1,m}$ is the average fuel temperature at elevation m. In this case, Eq. (24) becomes:

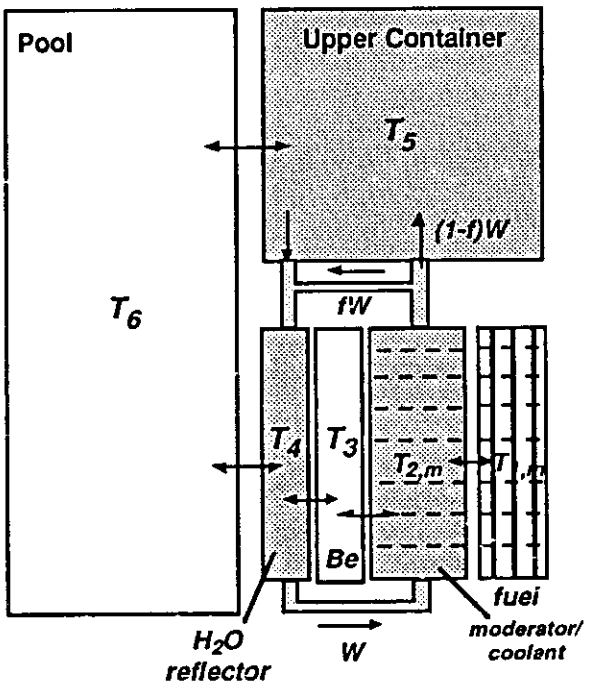

Figure 6: Temperature Model for SLOWPOKE–2

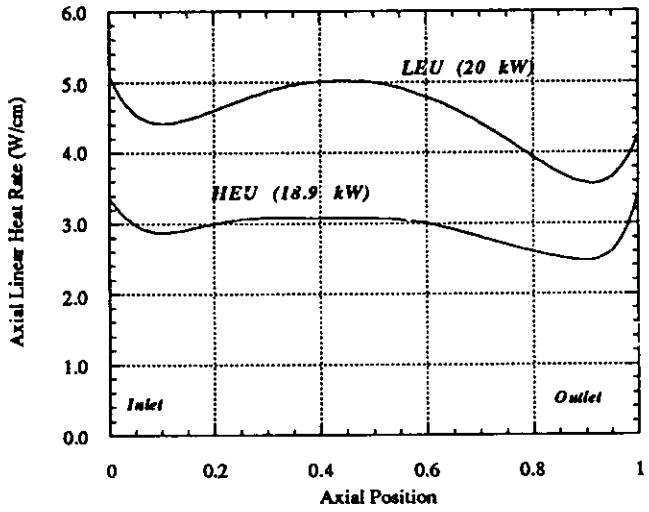

Figure 7: Axial Linear Heat Rate Distribution for SLOWPOKE–2 (full power)

$$k_f\,(T_{1,m})\,[T_{1,m} - T_{sm}] = \frac{q_m}{8\pi}\ , \tag{26}$$

where it was assumed that $T_{1,m} = (T_{sm} + T_{om})/2$.

The fuel surface temperature will be linked to the bulk coolant temperature $T_{2,m}$ by a thermal resistance, $R_{1,m}$, accounting for the fuel/sheath gap resistance ($h_{gap,m}$), for the sheath thermal conductivity (k_g) and for the heat transfer coefficient to the coolant ($h_{cal,m}$):

$$R_{1,m} = \frac{1}{2\pi r_f h_{gap,m}} + \frac{1}{2\pi k_g} \ln\left(\frac{r_s}{r_f}\right) + \frac{1}{2\pi r_s h_{cal,m}} \tag{27}$$

where r_f and r_s are the inner and outer radius of the fuel sheath, respectively.

The *gap resistance* is negligeable for HEU, while for LEU it is significant yet *uncertain*. The LEU sheath is free standing at full power. Gap thickness is expected to vary from one pin to the other, so that values ranging from 5 to 20 $kW/m^2/°C$ are suggested in the Safety Report. To account for reduced gap resistance when the fuel expands with increasing power and comes in better contact with the fuel sheath, we have used the following relation in SLOWKIN for $h_{gap,m}$ with LEU fuel:

$$h^{LEU}_{gap,m}(t) = h_{gap,o} \cdot [1. + \frac{q_m(t)}{q_o}] \tag{28}$$

where q_o is the average linear heat rate at nominal full power. A value of $h_{gap,o} = 3.5$ $kW/m^2/°C$ was arbitrarily chosen. Combining with Eq. (26), we can finally write (at steady-state):

$$T_{1,m} - T_{2,m} = q_m \cdot R_{tot,m} \tag{29}$$

where the *total* thermal resistance is:

$$R_{tot,m} = R_{1,m} + \frac{1}{8\pi k_f\,(T_{1,m})} \tag{30}$$

This total resistance will be used in SLOWKIN to cast the time-dependent equation for the average fuel temperature in a lump model:

$$\frac{\kappa_{1,m}}{H_m} \cdot \frac{dT_{1,m}(t)}{dt} = q_m(t) - \frac{1}{R_{tot,m}}\,[T_{1,m}(t) - T_{2,m}(t)] \tag{31}$$

where $\kappa_{1,m}$ is the thermal capacity of the fuel, including the fuel sheath:

$$\kappa_{1,m} = [M_f C_{p-f}(T_{1,m}) + M_s C_{p-s}]/M \tag{32}$$

A constant thermal conductivity is assumed for HEU fuel. For the ceramic UO_2 fuel (LEU), thermal conductivity is much smaller and is strongly dependent on temperature (see Figure 8)[15]. Consequently, a significant temperature gradient may arise in the fuel, and the above lump model can miscalculate the average fuel temperature. As a result,

an option was programmed in SLOWKIN to obtain the radial temperature profile in the fuel pins by solving the heat conduction equation within the UO_2, using finite differences. The fuel temperature profile equations are of the form: [7]

$$\frac{dT_{1,m}^{(j)}}{dt} = a_{jm}T_{1,m}^{(j-1)} + b_{jm}T_{1,m}^{(j)} + c_{jm}T_{1,m}^{(j+1)} + Q_m^{(j)} \tag{33}$$

where $(j = 1, ..., J)$, $(m = 1, ..., M)$ and $T_{1,m}^{(J)} = T_{sm}$ is the fuel surface temperature. The surface temperature $T_{1,m}^{(J)}$ is related to the bulk coolant temperature $T_{2,m}$ through the thermal resistance $R_{1,m}$ in Eq. (27).

The core average fuel temperature to be used in Eq. (18) is then simply:

$$T_1(t) = \frac{1}{M}\sum_{m=1}^{M} T_{1,m}(t) \tag{34}$$

where $T_{1,m}$ is obtained either directly from Eq. (31), or by averaging the temperature over the fuel volume using the J points obtained from Eq. (33).

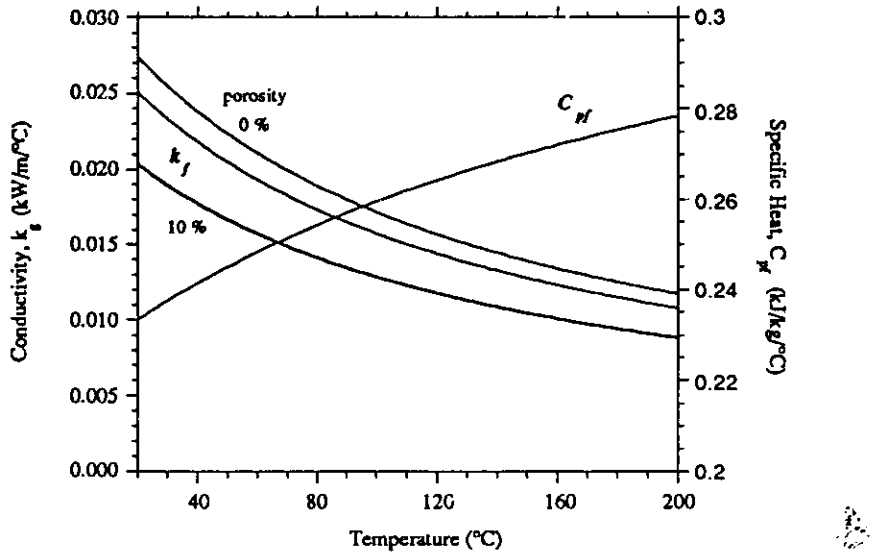

Figure 8: UO_2 Fuel Properties

In SLOWKIN simulations, we noted:

- Gap resistance can have a significant effect during the LEU transients because it determines the level of fuel temperature for a given power, and hence the level of negative feedback. We found that increasing the value of h_{gap} as in Eq. (28) produces a more pronounced prompt peak and a higher delayed power peak in LEU (since the resulting fuel temperature is lower);

- The UO_2 specific heat C_{p-f} affects the time constant associated with variations in fuel temperature. This time constant is of the order of a few seconds. Since power varies rather slowly beyond the prompt peak (if present), we found that the delayed peak power is not very sensitive to specific heat;
- The thermal conductivity affects the temperature gradient within the fuel pins, and determines the heat flux coming out of the fuel. A lower conductivity will tend to increase the fuel temperature, but we found this effect to be negligeable on the delayed peak power;
- The lump fuel model yields nearly identical results as the profile temperature model for HEU fuel. This is because the temperature is nearly uniform in the metallic fuel. Even for LEU fuel, with a much smaller conductivity, the lump model was found to be adequate, predicting nearly identical prompt and delayed peaks. This is because of the milder temperature gradient within the smaller fuel pins (compared to power reactors). The lump approximation is therefore valid even for fast transients.

2.3.2 Moderator/Coolant (T_2)

The thermal capacity of the moderator/coolant at level m in the core is:

$$\kappa_{2,m} = \frac{M_{mod} C_{p-mod}}{M} \quad ; \quad m = 1, ..., M \tag{35}$$

For region m, the coolant temperature equation can be written:

$$\begin{aligned} \kappa_{2,m} \frac{dT_{2,m}(t)}{dt} &= \frac{(1 - f_{rc})}{2} f_{\phi m} P(t) + \frac{N_c H_m}{R_{tot,m}} [T_{1,m}(t) - T_{2,m}(t)] \\ &\quad - h_{Be} A_{1,m} [T_{2,m}(t) - T_3(t)] + W \cdot [h_{e,m} - h_{s,m}] \quad , \end{aligned} \tag{36}$$

with:

$\frac{1-f_{rc}}{2}$ Fraction of fission energy deposited directly in region m of the moderator;

h_{Be} Convection heat transfer coefficient between the moderator/coolant and the interior of the berylium reflector $[\frac{kW}{m^2 C}]$;

$A_{1,m}$ Heat transfer area between the moderator/coolant and the interior of the berylium reflector at level m ;

W Natural circulation flow $[\frac{kg}{s}]$;

$h_{e,m}$ Enthalpy at the inlet of section m (liquid) $[\frac{kJ}{kg}]$;

$h_{s,m}$ Enthalpy at the outlet of section m (liquid) $[\frac{kJ}{kg}]$.

However, we know that at constant pressure, we have:

$$dh = C_p dT. \tag{37}$$

Thus, Eq. (36) can be written for $m = 1, ..., M$:

$$\begin{aligned}\frac{dT_{2,m}(t)}{dt} &= \frac{(1-f_{rc})}{2\cdot\kappa_{2,m}} f_{\phi m} P(t) + \frac{N_c H_m}{\kappa_{2,m}\cdot R_{tot,m}}[T_{1,m}(t) - T_{2,m}(t)] \\ &\quad - \frac{h_{Be}A_{1,m}}{\kappa_{2,m}}[T_{2,m}(t) - T_3(t)] + \frac{W\,C_p}{\kappa_{2,m}}[T_{2,m-1}(t) - T_{2,m}(t)] \quad , \end{aligned} \tag{38}$$

with the inlet coolant temperature $T_{2,0}(t) = T_4(t)$.

With the profile option of Eq. (33), Eq. (38) becomes:

$$\begin{aligned}\frac{dT_{2,m}(t)}{dt} &= \frac{(1-f_{rc})}{2\cdot\kappa_{2,m}} f_{\phi m} P(t) + \frac{N_c H_m}{\kappa_{2,m}\cdot R_{1,m}}[T^{(J)}_{1,m}(t) - T_{2,m}(t)] \\ &\quad - \frac{h_{Be}A_{1,m}}{\kappa_{2,m}}[T_{2,m}(t) - T_3(t)] + \frac{W\,C_p}{\kappa_{2,m}}[T_{2,m-1}(t) - T_{2,m}(t)] \quad , \end{aligned} \tag{39}$$

Finally, the core average moderator/coolant temperature to be used in Eq. (18) is simply:

$$T_2(t) = \frac{1}{M}\sum_{m=1}^{M} T_{2,m}(t) \tag{40}$$

2.3.3 Berylium Reflector (T_3)

$$\kappa_3 = M_{be} C_{p-be} \tag{41}$$

$$\kappa_3 \frac{dT_3(t)}{dt} = h_{Be}A_1[T_2(t) - T_3(t)] - h_{Be}A_2[T_3(t) - T_4(t)] + \frac{1-f_{rc}}{4}P(t) \quad , \tag{42}$$

with:

$\frac{1-f_{rc}}{4}$ Fraction of fission energy deposited directly in the berylium reflector;

h_{Be} Heat transfer coefficient between coolant/berylium (A_1) or berylium/container water (A_2), $[\frac{kW}{m^2 C}]$;

2.3.4 Water Reflector (T_4)

$$\kappa_4 = M_{ref} C_{p-ref} \tag{43}$$

$$\begin{aligned}\frac{dT_4(t)}{dt} &= \frac{h_{B2}A_{B2}}{\kappa_4}[T_3(t) - T_4(t)] - \frac{h_{RP}A_{RP}}{\kappa_4}[T_4(t) - T_6(t)] \\ &+ \frac{WC_p}{\kappa_4}[(1 - f_{rec})T_5(t) + f_{rec}T_{2,M}(t) - T_4(t)] + \frac{1 - f_{rc}}{4\kappa_4}P(t) \quad , \end{aligned} \tag{44}$$

where:

$\frac{1-f_{rc}}{4}$ Fraction of fission energy deposited directly in the water reflector;

h_{RP} Global heat transfer coefficient between the reactor container and the pool. This coefficient was adjusted to yield the observed behaviour of the container water temperature at constant power over the long term (hours). The same value (0.2 $\frac{kW}{m^2C}$) applies to both HEU and LEU;

f_{rec} Recirculation fraction; a fraction $f_{rec}W$ flows directly into the downcomer (see Fig. 6). It is expected that this fraction *increases* with flow rate, as an increasing flow in the downcomer entrains a larger fraction of the hot water comming out of the outlet orifice. In SLOWKIN, we have assumed that $f_{rec} = aW^2$, with $a = 2.5$.

2.3.5 Upper Reactor Container Water (T_5)

$$\kappa_5 = M_{cont} C_{p-cont} \tag{45}$$

$$\frac{dT_5(t)}{dt} = \frac{(1 - f_{rec})W\,C_p}{\kappa_5}[T_{2,M}(t) - T_5(t)] - \frac{h_{CP}A_{CP}}{\kappa_5}[T_5(t) - T_6(t)] \quad , \tag{46}$$

where $T_{2,M}(t)$ is the core outlet coolant temperature. A fraction $(1 - f_{rec})W$ flows directly into the upper container.

2.3.6 Pool Water (T_6)

$$\kappa_6 = M_{pool} C_{p-pool} \tag{47}$$

$$\frac{dT_6(t)}{dt} = \frac{h_{RP}A_{RP}}{\kappa_6}[T_4(t) - T_6(t)] + \frac{h_{CP}A_{CP}}{\kappa_6}[T_5(t) - T_6(t)] \quad . \tag{48}$$

where heat removal from the pool has been neglected.

2.4 Heat Transfer and Subcooled Nucleate Boiling

2.4.1 Natural Circulation

Let us suppose the reactor is just critical at very low power (a few watts). Temperature is essentially uniform at ambiant temperature throughout the assembly. The control rod is then removed, the reactor becomes supercritical and fission power increases. At one point, thermal power becomes significant and the fuel heats up. A few seconds later, heat is transfered to the moderator, which itself heats up. The density of the water in the core will begin to slowly decrease as the water temperature goes up. This local density change will evacuate some of the cooler water from the core (at both ends). On the other hand, when sufficient energy has been delivered to the moderator, buoyancy forces due to the lower water density in the core will start to act and will set the water in motion in a natural circulation pattern within the reactor container. In SLOWKIN, the steady state flow W is calculated in the following manner.

If power in the reactor is maintained at a constant level, a fixed natural circulation flow will eventually be established. This *steady state flow* is the result of an equilibrium between the driving pressure difference (the buoyant driving force, Δp_d) and the pressure losses due to friction (Δp_f), acceleration (Δp_a) and viscous forces due to sudden changes in the geometry (mostly the inlet and outlet orifice areas, Δp_{inlet} and Δp_{outlet}). There is also a (small) loss term due to the abrupt change in flow direction at the core outlet. We therefore have:

$$\Delta p_d = \Delta p_f + \Delta p_a - \Delta p_{inlet} + \Delta p_{outlet} + \Delta p_{bend} \tag{49}$$

The driving pressure is only function of the elevation (core height, H_c) and the water density difference between inlet (ρ_1) and outlet (ρ_2):

$$\Delta p_d = (\rho_1 - \rho_2) g H_c \tag{50}$$

Pressure losses will be evaluated over three seperate sections of a simplified geometry, including the inlet section (flow area A_1), the core section (A_c) and the outlet section (A_2). We have:[17]

Friction losses

$$\Delta p_f = (\sum_j \frac{f_j H_j}{D_{hj} \rho_j A_j^2}) \cdot W^2 \tag{51}$$

where the friction factor is given by:

$$\begin{aligned} f_j &= \frac{64}{Re_j} \quad \text{for } Re_j < 2000 \text{ (laminar)} \\ &= \frac{0.184}{Re_j^{0.2}} \quad \text{else (turbulent)} \end{aligned} \tag{52}$$

The Reynolds number is obtained from:

$$Re_j = \frac{D_{hj} W}{A_j \mu} \ ,$$

with the hydraulic diameter given by $D_{hj} = \frac{4A_j}{P_{wj}}$ where P_{wj} is the *wetted perimeter* of the section.

As shown in Fig. 3, the inlet orifice is created by the seperation (δ_1) between the lower and latteral berylium reflectors. If R_c is the core radius, this determines the inlet orifice flow area:

$$A_1 = 2\pi R_c \delta_1 \tag{53}$$

The wetted perimeter is simply $P_{w1} = 2 \cdot (2\pi R_c + \delta_1) \approx 4\pi R_c$ so that

$$D_{h1} \approx 2\delta_1 \tag{54}$$

Using a similar approach for the outlet section, the values shown in Table 7 are obtained for the SLOWPOKE-2 reactor at École Polytechnique. In SLOWKIN simulations, it was found that *flow is laminar everywhere for reactor powers below 40 kW*. It becomes turbulent in the outlet section above this power level.

Table 7: Inlet and outlet orifices for SLOWPOKE–2 in SLOWKIN

orifice	Inlet	Outlet
D_h	1.120 cm	1.276 cm
A_j	38.7 cm^2	44.1 cm^2

Core values of hydraulic diameter are significantly different between LEU and HEU (3.44 cm vs. 2.28 cm), because of the fewer fuel pins in LEU.

Acceleration pressure drop

Acceleration pressure drop is due to expansion of the fluid in the core because of heating. It is usually small in single-phase flow. We have:

$$\Delta p_a = \left(\frac{1}{\rho_2} - \frac{1}{\rho_1}\right) \cdot \frac{W^2}{A_c^2} \tag{55}$$

Pressure drop at restrictions

Sudden changes in flow area at orifices cause kinetic-energy changes. A pressure *rise* occurs at the inlet orifice due to the expansion in flow area:

$$\Delta p_{inlet} = \left(\frac{1}{A_1 A_c} - \frac{1}{A_c^2}\right) \cdot \frac{W^2}{\rho_1} \tag{56}$$

At the outlet, a pressure *drop* occurs due to the sudden contraction:

$$\Delta p_{outlet} = 0.7 \left(\frac{1}{A_c^2} - \frac{1}{A_2^2}\right) \cdot \frac{W^2}{\rho_2} \tag{57}$$

Even if the flow area were recovered at the outlet (i.e. if $A_2 = A_1$), the pressure would *not* be recovered. The factor 0.7 accounts for this (actually representing a 40% loss in kinetic energy from the *vena contracta*).

Pressure drop due to change in flow direction

Finally, a small correction can be introduced to account for losses due the change in flow direction at the core outlet:

$$\Delta p_{bend} = \left(\frac{K_b}{2A_c^2}\right) \cdot \frac{W^2}{\rho_2} \tag{58}$$

where a value of $K_b = 0.6$ is recommended for a 90 ° bend.

We note that every term in the RHS of Eq. (49) is related to the kinetic energy of the fluid and is a function of the flow rate squared W^2. For a fixed geometry, there is therefore a fixed relationship between the natural circulation flow W and the power level P in the reactor, which is the determining factor for the fluid densities appearing in the above relations (ρ_1, ρ_c and ρ_2). Eq. (49) could therefore be written:

$$\Delta p_d = a[P] \cdot W^2 \tag{59}$$

Thus, we can write finally for the natural circulation flow rate:

$$\begin{aligned} W &= f_W[P] \\ &= \sqrt{\frac{\Delta p_d}{a[P]}} \end{aligned} \tag{60}$$

Since $P = WC_p\Delta T$, this translates into a fixed relationship between the power P and the water temperature ΔT across the core, which is measured in all SLOWPOKE reactors. Indeed, with very similar inlet and outlet orifices, the measured ΔT as a function of power is very similar for all SLOWPOKE reactors, as reported in the safety report.[8]

The above model assumes unidimensional flow and is a very simplified representation of the SLOWPOKE geometry. We expect this model to overestimate the flowrate. However, the model does contain the basic features of the geometry. In order to produce reasonable values of the flow rate in SLOWKIN, a constant correction factor was introduced in Eq. (60) to yield the observed core ΔT at full power (a correction factor of 0.75 was needed to produce a ΔT of approx. 20 °C at 20 kW).

The resulting relationship $W = f_W[P]$ is shown in Figure 9.

Eq. (60) is valid at *steady state*. When power varies during a transient, the instantaneous flow rate takes a certain time to develop, depending on the energy delivered to the coolant (rather than the instantaneous power in the fuel). The detailled hydrodynamics of natural circulation flow in a complex geometry such as the SLOWPOKE core can become quite involved. A major simplification was introduced in SLOWKIN which avoids solving for the conservation of momentum. The simplicifation is based on the following observation: during reactor transients in all SLOWPOKE reactors, a delay of approximately

10-20 s following a prompt peak has been observed before the outlet temperature begins to rise.[16]

To simulate this response in SLOWKIN, we will introduce a sampled first order filter with a time constant τ_f. The filtered response will be found as follows. Let x_n be the *unfiltered* response at time t_n, i.e. $x_n = f_W[P(t_n)]$. Then the *filtered* response, $W(t_n) = y_n$, will be:

$$y_n = a \cdot y_{n-1} + b \cdot (x_n + x_{n-1})/2. \tag{61}$$

with

$$a = e^{-\Delta t/\tau_f} \quad \text{and} \quad b = 1. - a \tag{62}$$

and where $\Delta t = t_n - t_{n-1}$.

The use of the steady state Eq. (60) with the above first order filter is a major simplification in SLOWKIN. It avoids the complex transient thermalhydraulics equations required to satify the principle of conservation of momentum, but yet it should capture the essence of the flow transient. In view of the observed delays in SLOWPOKE, a value of $\tau_f = 20s$ was used in all SLOWKIN simulations reported in section 3.

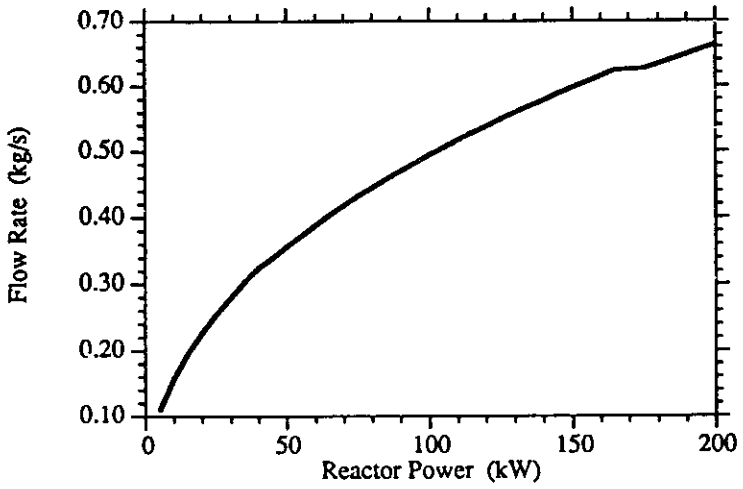

Figure 9: Natural Circulation Flow Rate in SLOWPOKE at Steady State

2.4.2 Heat Transfer Coefficient and ONB

An important term in the preceding equations is the heat transfer coefficient h_{cal} between the fuel sheath and the bulk moderator/coolant. This coefficient will vary with local conditions of flow and temperature since coolant motion increases the rate of heat transfer. If the wall (sheath) temperature remains below the liquid saturation temperature (in our case, 112°C), the single-phase coefficient h_{cal} must be determined.

A) Single-Phase Natural Convection

A well-established theory has been developed for single-phase free convection in the laminar boundary-layer regime.[18, 19] A variety of empirical and semi-empirical correlations are available for vertical cylinders.

The following non-dimensional numbers are defined:

Nusselt number: $\overline{\mathrm{Nu}}_H = \frac{h_{cal} \cdot H}{k}$

Prandtl number: $Pr = \frac{\mu C_p}{k}$

Rayleigh number: $\mathrm{Ra}_H = \frac{g\rho^2 C_p \beta \Delta T_{cal} H^3}{\mu k}$

where the temperature difference $\Delta T_{cal} = (T_S - T_\infty)$ is between the sheath and the bulk coolant. H is the cylinder height, μ is the water viscosity, k is the conductivity, g is the gravitational acceleration, and β is the coefficient of volumetric thermal expansion.

When the thermal boundary layer thickness δ_T is much smaller than the cylinder diameter D, the curvature of the lateral surface does not play a role in the heat transfer and the Nusselt number can be calculated with vertical wall formulas. In that case, if it can be verified that:

$$\frac{D}{H} \gg \mathrm{Ra}_H^{-\frac{1}{4}} \quad , \tag{63}$$

then the Churchill and Chu correlation can be used to find the wall-averaged Nusselt number for the entire Rayleigh number range (laminar, transition, and turbulent):[18]

$$\overline{\mathrm{Nu}}_H = \left\{ 0.825 + \frac{0.387 \mathrm{Ra}_H^{1/6}}{\left[1 + (0.492/\mathrm{Pr})^{9/16}\right]^{8/27}} \right\}^2 \tag{64}$$

This correlation holds true for $10^{-1} < \mathrm{Ra}_H < 10^{12}$ and for all Prandtl numbers.

When the inequality Eq. (63) is not valid, then the correlation developed by Lefevre and Ede can been used:

$$\overline{\mathrm{Nu}}_H = \frac{4}{3} \left[\frac{7 \mathrm{Ra}_H \, \mathrm{Pr}}{5\,(20 + 21\,\mathrm{Pr})} \right]^{1/4} + \frac{4\,(272 + 315\,\mathrm{Pr})\,H}{35\,(64 + 63\,\mathrm{Pr})\,D} \tag{65}$$

For the size of the fuel pins in SLOWPOKE, we find that Eq. (64) generally applies. Thus, the single-phase heat transfer coefficient at axial position m is:

$$h_{SP,m} = \overline{\mathrm{Nu}}_H \cdot \frac{k_m}{H} \tag{66}$$

where the Nusselt number is function of the wall ΔT, i.e. the temperature difference between the fuel sheath and the bulk coolant: $\Delta T_{cal,m} = T_{S,m}(t) - T_{2,m}(t)$.

B) Subcooled Nucleate Pool Boiling

When the temperature of fuel sheath becomes slightly higher than the water saturation temperature, subcooled nucleate boiling takes place. With Onset of Nucleate Boiling (ONB), vapor forms locally at nucleation sites on the heating surface. Bubbles form in small cavities and grow at these sites. Since the coolant is subcooled, the vapor bubbles normally recondense in the liquid, giving rise to no net evaporation. If subcooling is high, the bubbles may not even detach from the wall. In any case, heat transfer is improved by the fluid motion near the wall.

As the fuel surface temperature is increased, vaporization will continue and more bubbles will form on the fuel surface at nucleation sites. Both the frequency of bubbles collapse or detachment and the number of nucleation sites will increase with the wall superheat, $\Delta T_{wall} = T_{wall} - T_{sat}$.

Therefore, once ONB is reached, heat transfer is dramatically improved. In this regime, the heat flux becomes a function of the wall superheat alone, independent of the subcooling (or the subcooled liquid temperature):

$$q''_{NB} = h_{NB} \cdot (T_S - T_{sat}) \quad . \tag{67}$$

In SLOWKIN, we have used the correlation proposed by Rohsenow for the subcooled nucleate boiling regime.[21] This correlation can be written:

- When the heat flux q''_{NB} is known, the wall (sheath) temperature can be obtained from:

$$T_S - T_{sat} = \frac{h_{fg}}{C_p} (\mathrm{Pr})_l^s \, C_{sf} \left[\frac{q''_w}{\mu_l h_{fg}} \left(\frac{\sigma}{g\,(\rho_l - \rho_v)} \right)^{\frac{1}{2}} \right]^{1/3} . \tag{68}$$

  This correlation applies to clean surfaces and it is insensitive to shape and orientation of the surface. The empirical constant C_{sf} accounts for the particular combination of liquid and surface material, the exponent s, differentiates only between water and the other liquids, the subscripts l, v denote saturated liquid and saturated vapor. The symbol σ denotes the surface tension of the liquid in contact with its own vapor. Finally, h_{fg} is the latent heat of vaporization.

- Alternatively, when the wall (sheath) temperature is known, the Rohsenow correlation yields the nucleate boiling heat flux:

$$q''_{NB} = \mu_l h_{fg} \left(\frac{g(\rho_l - \rho_v)}{\sigma} \right) \left[\frac{C_p (T_S - T_{sat})}{\mathrm{Pr}_l^s \, C_{sf} \, h_{fg}} \right]^3 . \tag{69}$$

Considering Eq. (67), the nucleate boiling heat transfer coefficient can be written:

$$h_{NB} = \mu_l h_{fg} \left(\frac{g(\rho_l - \rho_v)}{\sigma} \right) \left[\frac{C_p}{\mathrm{Pr}_l^s \, C_{sf} \, h_{fg}} \right]^3 (T_S - T_{sat})^2 . \tag{70}$$

The heat flux from the fuel at position m can therefore be written:

$$\begin{aligned} q''_m(t) &= h_{cal,m} \cdot \Delta T_{cal,m} && (71) \\ &= h_{SP,m} \cdot (T_{S,m} - T_{2,m}) + h_{NB,m} \cdot (T_{S,m} - T_{sat}) && (72) \end{aligned}$$

During transients in SLOWKIN, the instantaneous heat flux is given by the temperature difference between *fuel* and the coolant, using thermal resistance R_1 in Eq. (27). The heat transfer coefficient $h_{cal,m}$ and the *sheath* temperature $T_{S,m}$ are obtained simultaneously. *Onset of Nucleate Boiling* (ONB) occurs when $T_{S,m}$ exceeds the saturation temperature (T_{sat}).

We note in Figure 10 that the heat transfer coefficients obtained with the Rohsenow correlation are quite sensitive to the surface constant C_{sf}. Values given in the litterature range between 0.006 and 0.013 for stainless steel and water,[18] depending on the quality of the surface (a more polished surface will bear fewer nucleation sites). For SLOWPOKE-2, we have arbitrarily assigned the values given in Table 8, considering the zircalloy sheath in LEU to be equivalent to industrial stainless steel. For HEU, we assumed a somewhat smaller value of C_{sf} for the aluminium sheath, because of its better conductivity and more porous surface. The resulting heat transfer coefficient is illustrated in Figure 11.

Table 8: Surface C_{sf} for SLOWPOKE–2

core	C_{sf}
HEU	0.0060
LEU	0.0045

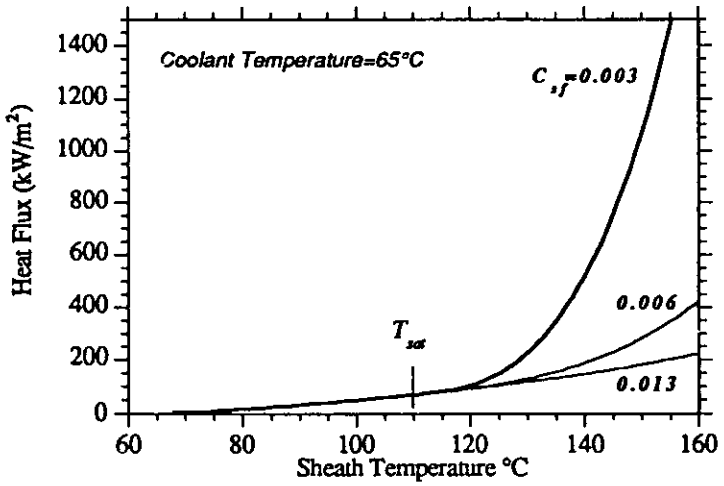

Figure 10: Influence of Surface C_{sf} on Nucleate Boiling Heat Transfer

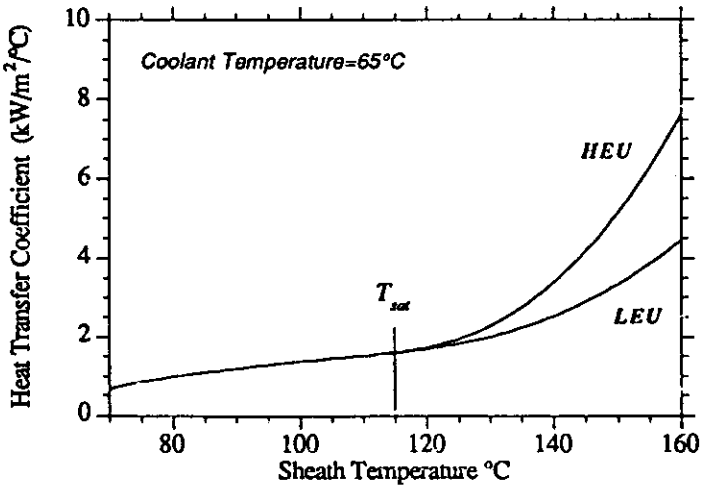

Figure 11: Heat Transfer Coefficient for SLOWPOKE–2

2.4.3 Void Fraction

A) Wall Voidage

The subcooled nucleate boiling regime can be considered to be *partially developped* when bubbles remain attached to the wall (wall voidage). With increasing wall temperature, the bubbles grow beyond a critical size and detach from the wall. Once bubble detachment occurs, subcooled nucleate boiling is *fully developped* and more significant void fractions occur.

Although the void fraction is quite small before bubble detachment, it cannot be neglected because of the very large negative void coefficient in SLOWPOKE (ex. a void fraction only 1% is worth almost as much as the control rod). An approximate model of the flow in this regime was developped by Griffith. For highly subcooled flow boiling at moderate pressures, the following correlation is proposed for the void fraction:[24]

$$\alpha_m = 3.73 \frac{q''_{NB,m}}{h_{SP}[T_{sat} - T_{2,m}]} \left(\frac{k_\ell}{h_{SP} D_h} \right) Pr_\ell \tag{73}$$

where D_h is the hydraulic diameter ($= 4S/P$). *Thus, in the partial nucleate boiling regime, the void fraction is a function of the local conditions alone*: it increases with wall superheat, and it decreases with increasing subcooling. We note that because of the smaller number of pins, the hydraulic diameter is larger in LEU (4.2 cm vs 2.6 cm) so that smaller void fractions are expected (all else being equal).

B) Detached Voidage

Beyond the point of bubble detachment, the modeling efforts invariably require knowledge of how the bubble frequency, departure diameter and density of active nucleation sites vary with wall superheat. Despite years of research, these aspects of the boiling process are not well understood.[20]

A succesful alternative to mechanistic modelling is the profile-fit model of Zuber.[22] Let X_e be the thermodynamic quality (negative in the subcooled domain). At elevation z in the core, we can calculate it simply as:

$$X_e = \frac{C_p [T_2(z) - T_{sat}]}{h_{fg}} \tag{74}$$

Let X_e^d be the *thermodynamic quality* at the point of bubble detachment. Then the *true quality* (always positive) is given by:

$$X = X_e - X_e^d \cdot e^{\left[\frac{X_e}{X_e^d} - 1\right]} \tag{75}$$

The void fraction is then obtained with the void-quality relation:

$$\alpha_m = \frac{X}{X + S \cdot \frac{\rho_g}{\rho_\ell}[1 - X]} \tag{76}$$

where S is the slip ratio.

The most important part of any effective subcooled boiling model is to be able to calculate accurately where significant void fractions appear, i.e. *the void departure point.* As water flows up the core, subcooling is gradually reduced, and could reach a critical subcooling at which bubble detachment occurs. The following critical subcooling criteria have been proposed by Saha and Zuber for predicting the point of bubble detachment:

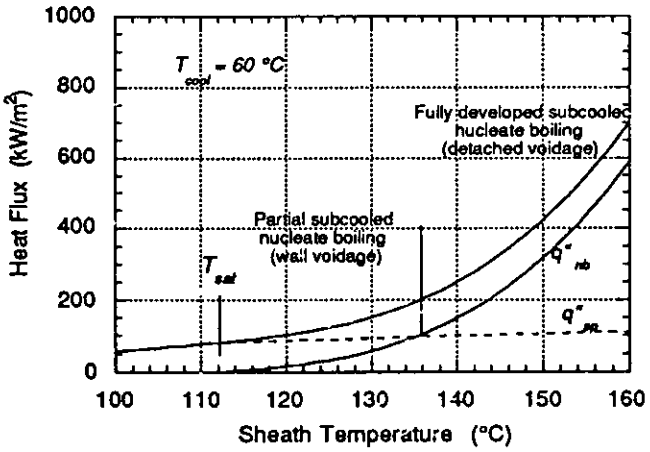

Figure 12: Subcooled Nucleate Boiling Regimes

- At low mass fluxes, bubble detachment depends only on local thermal conditions which determine the rates of vapour formation at the wall (proportional to the heat flux) and the rate of condensation (proportional to the local subcooling). For *thermally controlled detatchment*, when the Peclet number $Pe = GD_H C_p/k < 70000$, the following criterion for critical subcooling is used:

$$\Delta T_{sub} = 0.0022 \frac{q'' D_H}{k} \tag{77}$$

- At high mass fluxes ($Pe > 70000$), where mechanistic bubble detachment models are succesful, the process is *hydrodynamically controlled.* We have:

$$\Delta T_{sub} = 154 \frac{q''}{GC_p} \tag{78}$$

G is the mass flux. Pe is of the order of 2000-3000 in SLOWPOKE so that bubble detachment is clearly thermally controlled, and Eq. (77) generally applies. We note finally that for the low pressure found in the SLOWPOKE, the void-quality relation (Eq. (76)) produces a large void fraction for a small steam quality. Considering the large void coefficient, it would then be *very unlikely that detached voidage is ever achieved in SLOWPOKE-2*, unless a significant prompt peak is present.

C) Core Average Void Fraction

In the temperature model described in the previous section, the axial distribution of coolant temperature, $T_{2,m}(t)$, is obtained from the heat balance equation for an *average* fuel pin, since Eq. (31) uses the *average* linear rating at elevation m.

As we have seen above, initial void formation in the reactor is dependent on local conditions: ONB depends strictly on the sheath temperature, and wall voidage up to bubble detachment depends on local wall superheat and subcooling. Consider for example a situation where the lump model predicts a sheath temperature equal to saturation temperature. The model will predict no void formation, while in reality, a significant number of fuel pins are operating at a higher than average linear rating because the radial neutron flux shape is not uniform, and therefore sheath temperatures *above* the saturation temperature will be produced. The average pin calculation (lump) thus tends to underestimate the initial void formation in the core.

The distributions of pin power (relative to the average) for the HEU and LEU cores are shown in Figures 13 and 14. These were obtained from the 3D diffusion calculations in DONJON [13] and will be assumed fixed during the transients. The following assumptions are made to account for the nonuniform radial distribution of pin powers in our prediction of the core-average void fraction.

- The axial distribution of coolant temperature $T_{2,m}(t)$ is given by the average pin calculation described in Section 2.3. It is assumed to apply to all fuel pins;
- An histogram of the radial power distribution in the reactor is given at input to SLOWKIN, providing the number of pins for each power interval as shown in Figures 14 and 15 (in this case, 10 intervals were used);
- Seperate *slave* calculations of fuel and fuel sheath temperatures will be carried out for the different pin powers at each elevation, imposing the coolant temperature $T_{2,m}(t)$ as a boundary condition at each elevation;
- The void profile is calculated for each group of fuel pins using the above correlations and a volume average of the void fraction is then calculated. This core average value is fed back into Eq. (19).

Thus core average void fraction will be given by:

$$\alpha(t) = \frac{1}{M} \sum_{m=1}^{M} \sum_{j=1}^{J} f_j \alpha_{m,j}(t) \tag{79}$$

with:

$\alpha_{m,j}$ Void fraction calculated in the j'th slave calculation at elevation m;

f_j The fraction of fuel pins in slave group j.

2.4.4 Critical Heat Flux

During transients, the *average* heat flux from the fuel pins is calculated at each level m using Eq. (72). As we have seen previously, power is not uniform radially in the core. The detailled 3D diffusion calculations in DONJON have also provided the ***radial form factors*** given in Table 9. The radial form factors are defined as the ratio of maximum pin power to average pin power in the reactor.

The critical heat flux in SLOWPOKE-2 can be estimated by:[8]

$$CHF_m(t) = 580 + 11 \cdot \Delta T_{sub}(t) \tag{80}$$

$$= 580 + 11 \cdot [T_{sat} - T_{2,m}(t)] \tag{81}$$

where CHF is in $[kW/m^2]$. The local heat flux, increased by the radial form factor, will be compared to the CHF:

$$CHFR_m(t) = \frac{CHF_m(t)}{f_{\text{rad}} \cdot q''_m(t)} \tag{82}$$

Finally, the *minimum critical heat flux ratio* for a transient is obtained:

$$MCHFR = \min_{\{m,t\}} CHFR_m(t) \tag{83}$$

Table 9: DONJON Form Factors for SLOWPOKE–2

core	f_{rad}	f_{ax}	f_{tot}
HEU	1.261	1.0635	1.341
LEU	1.554	1.1190	1.739

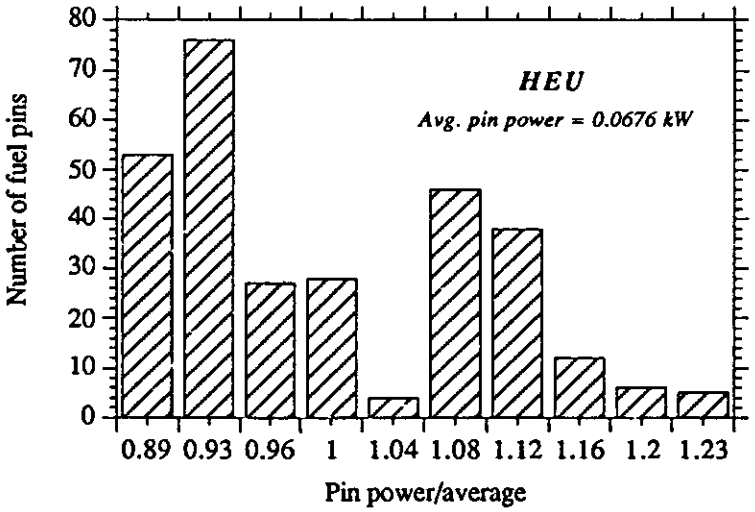

Figure 13: Distribution of pin power relative to average in HEU calculated in DONJON

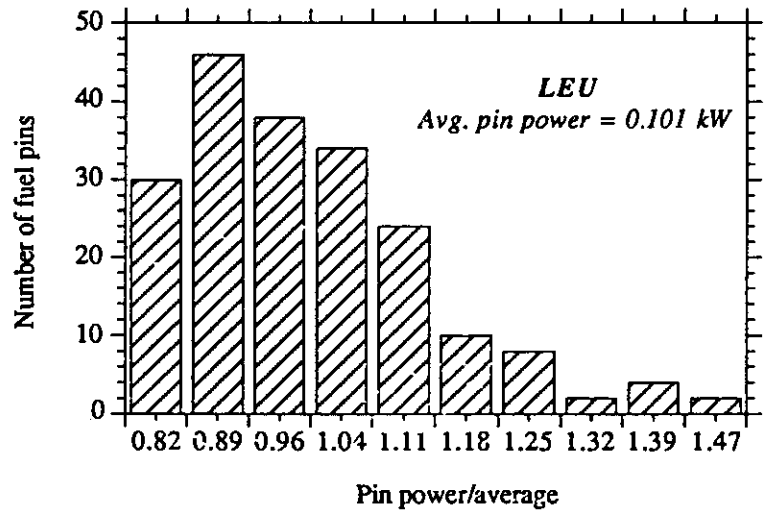

Figure 14: Distribution of pin power relative to average in LEU calculated in DONJON

3. SLOWKIN SIMULATIONS

We will now present some results obtained with SLOWKIN for the École Polytechnique SLOWPOKE-2 reactor. The input data is reproduced in Appendix B. Three types of simulations were carried out, similar to the proposed commissionning tests. All calculations were carried out starting with xenon-free fuel, at a *reference temperature* of 20 °C for the pool and container water.

3.1 Core Heating Effects

For these simulations, the reactor is started up and brought rapidely to a given power level (neutron power). The reactivity change due to the temperature increase is compensated (and measured) by automatic control rod displacements. The values reported in Tables 10 and 11 were calculated 10 minutes after startup from zero power (a period of approximately 5 minutes is required for the control rod position to stabilize).

We note that eventhough LEU posesses a significant fuel temperature component, the core heating effects for LEU are approximately 30% *smaller* than in HEU. This is due to the significantly larger moderator reactivity coefficient in HEU (see coefficient a_{21} in Table 4).

Table 10: HEU Core Temperature Reactivity Effects (Constant Power, 10 minutes after startup)

P_{th}	*Fuel*		*Moderator*		*Be Reflector*		*Water Reflector*		*Control Rod*
(kW)	°C	*mk*	°C (out)	*mk*	°C	*mk*	°C (in)	*mk*	*mk*
1.835	27.77	0.007	26.58	-0.479	20.74	0.006	20.04	0.002	0.457
4.953	33.65	0.013	30.41	-0.776	21.32	0.011	20.13	0.005	0.757
9.181	40.87	0.019	34.70	-1.135	22.07	0.017	20.37	0.016	1.088
18.35	51.95	0.029	40.92	-1.724	23.45	0.028	21.20	0.050	1.621

Table 11: LEU Core Temperature Reactivity Effects (Constant Power, 10 minutes after startup)

P_{th}	*Fuel*		*Moderator*		*Be Reflector*		*Water Reflector*		*Control Rod*	**Measured**
(kW)	°C	*mk*	°C (out)	*mk*	°C	*mk*	°C (in)	*mk*	*mk*	**(RMC)**
1.940	30.36	-0.105	26.64	-0.181	20.76	0.002	20.04	0.002	0.288	0.24
4.862	38.90	-0.192	30.55	-0.307	21.36	0.003	20.14	0.006	0.493	0.44
9.718	49.52	-0.300	34.92	-0.472	22.17	0.005	20.42	0.017	0.746	0.68
19.43	65.65	-0.464	41.30	-0.767	23.60	0.008	21.35	0.053	1.176	1.17

3.2 Long-Term Operation

During long-term operation at constant power, the slow temperature increase in the reactor container forces the gradual withdrawl of the control rod. This was simulated with SLOWKIN and results are shown in Figure 15, for constant operation at full power (10^{12} n/cm^2/s) for a period of 6 hours. Again, we note that the reactivity compensation is *smaller* in LEU, because the moderator coefficient is smaller. This implies that for a given excess reactivity margin, *the LEU core will permit full power operation for a significantly longer period.*

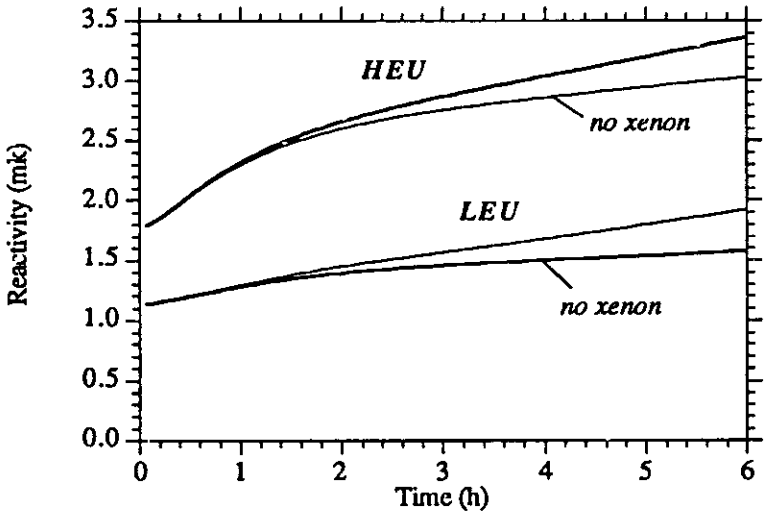

Figure 15: Reactivity Compensation at 100% Power

3.3 Self-limited Reactivity Transients

Self-limited reactivity transients occur when the control rod is removed from the reactor at low power. As noted before, a *prompt peak* will first appear as an inflexion in the early part of the transient, and will gradually form a distinct peak as the reactivity insertion is increased. The prompt peak can become quite large, and depends on fast acting feedback mechanisms (fuel temperature, coolant heating, and incipient void) when natural circulation flow has not fully developped. Beyond the prompt peak, a *delayed peak* is generally observed, when the flow is fully devellopped and the initial reactivity is completely compensated by the various feedback mechanisms described above.

Figures 16 and 17 show the reactivity transients calculated with SLOWKIN for HEU. Similar transients are shown for LEU in Figures 18 and 19. We note that in both cases, the prompt peak is not apparent for reactivity insertions below 4 mk. The maximum reactivity insertion contemplated for the commissionning tests of the new core at École Polytechnique is 4.3 mk. Even for this maximum available licensed excess reactivity, the prompt peak is hardly noticeable.

Tables 12 and 13 describe the core behaviour at the delayed peak. Only core averaged quantities are given. We note that for all transients considered, including the maximum licensed excess reactivity, margin to dryout is considerable (MCHFR). Tables 14 and 15 provide details of the reactivity compensation calculated in SLOWKIN for self-limited reactivity transients in HEU and LEU. Finally, the delayed peak power predicted by SLOWKIN is compared with experimental data in Figure 20 for both cases (Tunney's Pasture for HEU cores and RMC for LEU cores). As we can see, the anticipated behaviour for the SLOWPOKE reactor at École Polytechnique is fairly well predicted with SLOWKIN.

More specifically, we note:

- For reactivity insertions of 0-3 mk, the delayed peak power is *higher* in LEU than in HEU, due to a smaller negative reactivity coefficient of the core water (moderator/coolant) and a larger positive coefficient for the water oustide the core (reflector);
- Fuel temperature feedback plays a significant role in LEU, even for small perturbations. For example, at 2 mk, fuel temperature feedback represents 50 % of the negative component (see Table 15);
- For intermediate reactivities in the range 2-4 mk (0.25β to 0.5β), the feedback in HEU is still entirely limited to water temperature effects. In LEU however, negative void feedback becomes apparent. SLOWKIN simulations indicate that *Onset of Nucleate Boiling (ONB) occurs in LEU for transients above 2.8 mk. For HEU, ONB occurs for transients above 4.5 mk*:
  - there is a significant drop in power over a period of 10 minutes beyond the delayed peak. This reduction is due to the transient increase of inlet water temperature resulting from more mixing at the outlet orifice;
  - above 3 mk in LEU, void feedback plays an increasingly important role. Void feedback causes nearly 20% of the reactivity compensation at the delayed peak in the 4.3 mk transient (see Table 15);
  - beyond 4.5 mk, void feedback becomes the second most important feedback mechanism in LEU. In HEU, void feedback becomes significant beyond 5 mk;
- The *core average* void fraction is extremely small: even for the 4.3 mk transient in LEU, the maximum core-average void fraction is less than 0.2 %. For the 5 mk transient in HEU, it is less than 0.05 %. Tables 16 and 17 show the detailled void fraction distribution at the delayed peak for the 4.3 mk transient in LEU. We note

that the maximum local void fraction is 2.8 % in the hot pins, while there is no void in the cold pins. Bubble detachment (or so-called Onset of Significant Void) has not occured, because of the low flow and the very large subcooling (40 °C). This is still the case even in the 6 mk transients. Therefore, *void formation in LEU transients is entirely due to wall voidage.*

- In the 4-6 mk range (0.5β to 0.75β), a *prompt peak* appears in both LEU and HEU. Because of the prompt Doppler effect in LEU, the prompt peak is generally *smaller* than in HEU, where the fuel temperature feedback is negligeable (see table 4);
- for large reactivity insertions (above 0.7β), the delayed peak is nearly the same in HEU and LEU. Furthermore, as seen in Figure 20, the delayed peak power does not increase significantly with increasing reactivity. This is due to the dominating effect of void feedback at power levels above 100 kW.

A word of caution concerning Figure 20. We note that the experimental data was obtained for different SLOWPOKE-2 reactors which may exhibit differences with the reactor installed at École Polytechnique. These differences have not been analysed. Rather than speculating, we will wait for the actual commissionning measurements before making a detailled comparison. However, the trend suggested by Figure 20 is that SLOWKIN overpredicts the delayed peak beyond ONB. Considering the uncertainty in the wall voidage correlation (Eq. (73)), and the approximate treatment of the void coefficient (see section 2.2.3), the anticipated discrepancy in delayed peak power is not alarming.

Table 12: HEU-core Behaviour at Delayed Peak (core average)

Reactivity	*1 mk*	*2 mk*	*3 mk*	*4 mk*	*5 mk*	*6 mk*
peak power (kW)	7.082	25.83	49.35	69.83	93.94	99.08
time (min)	27.7	11.8	6.19	4.21	3.04	2.41
T_{inlet} (°C)	20.45	21.45	22.44	23.59	24.44	24.52
T_{outlet} (°C)	33.14	44.65	54.05	61.75	69.20	72.13
$T_{moderator}$ (°C)	27.46	34.22	39.82	44.54	48.98	50.60
T_{fuel} (°C)	37.98	59.07	77.26	90.82	104.44	109.62
T_{sheath} (°C)	37.94	58.92	76.98	90.43	103.92	109.04
void (%)	0.0	0.0	0.0	0.0	0.033	0.157
flow (kg/s)	0.128	0.256	0.357	0.420	0.481	0.503
MCHFR	179.24	46.63	23.12	15.19	10.48	8.53

Table 13: LEU-core Behaviour at Delayed Peak (core average)

Reactivity	*1 mk*	*2 mk*	*3 mk*	*4 mk*	*4.3 mk*	*5 mk*	*5.5 mk*	*6 mk*
peak power (kW)	13.95	41.62	69.06	85.96	89.42	96.31	100.59	103.98
time (min)	26.6	10.7	5.68	3.50	3.16	2.64	2.43	2.28
T_{inlet} (°C)	21.15	23.07	24.28	24.22	24.24	24.31	24.40	24.53
T_{outlet} (°C)	38.24	51.37	61.43	66.32	67.28	69.26	70.50	71.49
$T_{moderator}$ (°C)	30.66	38.77	44.87	47.53	48.06	49.17	49.89	50.49
T_{fuel} (°C)	57.37	92.52	118.55	132.05	134.57	139.31	142.07	144.18
T_{sheath} (°C)	52.14	81.67	100.30	114.21	116.20	119.89	122.01	123.61
void (%)	0.0	0.0	0.012	0.113	0.156	0.269	0.358	0.441
flow (kg/s)	0.188	0.338	0.426	0.468	0.476	0.491	0.500	0.507
MCHFR	47.28	14.86	8.51	6.65	6.36	5.84	5.55	5.32

Table 14: Reactivity Compensation (mk) at the Delayed Peak in HEU

Insertion (mk)	ρ_{fuel} *(mk)*	ρ_{mod} *(mk)*	ρ_{refl} *(mk)*	ρ_{void} *(mk)*	*Peak Power* (kW)
1.0 mk	0.016	-1.011	0.041	0.0	7.08
2.0 mk	0.036	-2.081	0.090	0.0	25.83
3.0 mk	0.053	-3.075	0.130	0.0	49.35
4.0 mk	0.065	-3.990	0.179	0.0	69.83
5.0 mk	0.077	-4.915	0.214	-0.165	93.94
6.0 mk	0.082	-5.268	0.217	-0.772	99.08

Table 15: Reactivity Compensation (mk) at the Delayed Peak in LEU

Insertion (mk)	ρ_{fuel} *(mk)*	ρ_{mod} *(mk)*	ρ_{refl} *(mk)*	ρ_{void} *(mk)*	*Peak Power (kW)*
1.0 mk	-0.380	-0.628	0.055	0.0	13.95
2.0 mk	-0.787	-1.343	0.132	0.0	41.62
3.0 mk	-1.002	-2.017	0.179	-0.053	69.06
4.0 mk	-1.139	-2.347	0.174	-0.498	85.96
4.3 mk	-1.165	-2.416	0.175	-0.686	89.42
5.0 mk	-1.213	-2.562	0.178	-1.180	96.31
5.5 mk	-1.241	-2.659	0.182	-1.571	100.59
6.0 mk	-1.262	-2.741	0.187	-1.930	103.98

Table 16: Axial Temperature Distribution in LEU for the 4.3 mk Insertion at the Time of Maximum Void (6.4 min)

plane	Tmod (°C)	Tsheath (°C)	Tfuel (°C)	void (%)	heat flux (kW/m2)	CHFR
15	67.921	123.267	139.677	0.197	96.107	7.130
14	65.599	119.909	135.658	0.066	90.877	7.721
13	63.406	120.274	136.632	0.071	96.253	7.451
12	61.079	121.425	138.753	0.097	104.392	7.028
11	58.550	122.376	140.572	0.120	112.362	6.689
10	55.823	122.749	141.683	0.124	119.072	6.474
9	52.928	122.474	141.939	0.107	124.036	6.380
8	49.909	121.486	141.265	0.076	126.983	6.400
7	46.815	119.806	139.610	0.040	127.846	6.528
6	43.699	117.258	136.881	0.012	126.702	6.762
5	40.611	114.010	133.239	0.001	123.775	7.098
4	37.593	110.209	128.876	0.000	119.456	7.533
3	34.682	106.337	124.420	0.000	114.714	8.025
2	31.886	103.421	121.175	0.000	112.222	8.379
1	29.151	104.221	122.681	0.000	118.779	8.080

Table 17: Void Distribution in % for the 4.3 mk Insertion in LEU (Slave Calculation)

slave group	1	2	3	4	5	6	7	8	9	10
no pins	30	46	38	34	24	10	8	2	4	2
power/avg.	0.825	0.894	0.965	1.037	1.108	1.179	1.251	1.322	1.393	1.465
PLANE 15	0.001	0.024	0.104	0.266	0.510	0.841	1.247	1.713	2.232	2.812
14	0.000	0.001	0.026	0.103	0.253	0.475	0.777	1.141	1.561	2.031
13	0.000	0.001	0.028	0.110	0.270	0.507	0.819	1.194	1.622	2.113
12	0.000	0.004	0.042	0.150	0.338	0.611	0.960	1.371	1.836	2.359
11	0.000	0.006	0.056	0.181	0.393	0.692	1.065	1.500	1.998	2.543
10	0.000	0.007	0.058	0.191	0.412	0.718	1.102	1.547	2.052	2.603
9	0.000	0.004	0.048	0.172	0.384	0.682	1.058	1.497	1.993	2.535
8	0.000	0.001	0.031	0.130	0.318	0.591	0.942	1.357	1.830	2.349
7	0.000	0.000	0.013	0.079	0.226	0.459	0.772	1.145	1.581	2.064
6	0.000	0.000	0.002	0.032	0.130	0.307	0.563	0.883	1.267	1.701
5	0.000	0.000	0.000	0.006	0.052	0.166	0.356	0.616	0.930	1.305
4	0.000	0.000	0.000	0.000	0.010	0.064	0.183	0.368	0.615	0.917
3	0.000	0.000	0.000	0.000	0.000	0.014	0.072	0.190	0.367	0.602
2	0.000	0.000	0.000	0.000	0.000	0.002	0.027	0.101	0.232	0.420
1	0.000	0.000	0.000	0.000	0.000	0.005	0.043	0.137	0.291	0.502

4. CONCLUSION

A simplified model was developed to simulate the transients occuring in the SLOWPOKE-2 reactor due to control rod movements. The SLOWKIN code described in this report was used to simulate transients which will be measured during the commissionning of the new LEU core at École Polytechnique. For LEU, these pre-simulations are subject to a number of uncertainties, relating mostly to:

- the reactivity coefficients used in SLOWKIN. These are best estimates obtained by detailled neutronic modelling of the reactor using DRAGON/DONJON with the ENDF/B5 cross section library;
- the natural circulation flow rate and the degree of coolant mixing at the reactor outlet as a function of power;
- the reactivity effect of the water surrounding the core;
- the unknown gap resistance in the fuel;
- onset of nucleate boiling (ONB) which has a significant effect on the convection heat transfer to the moderator;
- the importance of void formation at high power, which rapidly becomes the limiting feedback mechanism for larger reactivity insertions;

It is expected that comparisons with the commissionning data at École Polytechnique will enable us to reduce some of the above uncertainties and provide us with a reasonable degree of confidence in the modelling approach. The SLOWPOKE 2 reactor is designed with a limited amount of excess reactivity. With our SLOWKIN model, we can extrapolate beyond this range. According to this model, power is self limited in large reactivity transients (up to 0.75β), providing a still very significant margin to dryout ($MCHFR > 5$). With the expected large value of the negative void coefficient, of the order of 4 mk /%, it is unlikely that the critical heat flux would ever be reached during the delayed peak, even for reactivities approaching prompt critical. Of course, in that virtual situation, the prompt peak would be much larger and fuel integrity may be questionned.

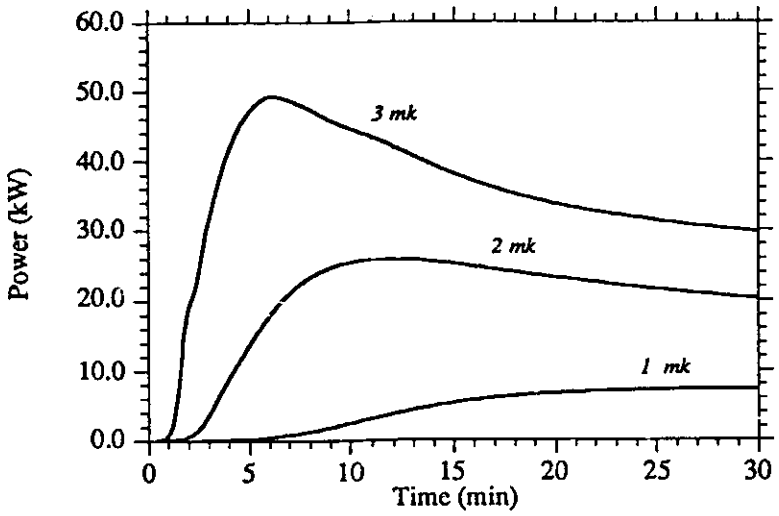

Figure 16: Self-limited Reactivity Transients in HEU (1-3 mk)

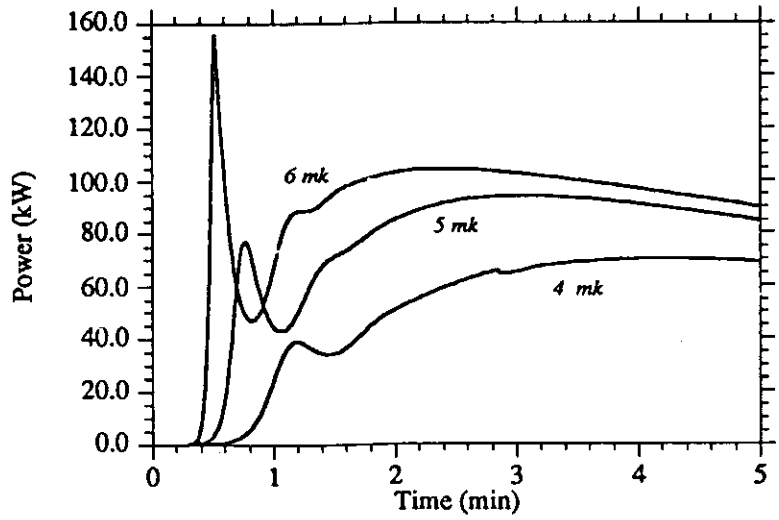

Figure 17: Self-limited Reactivity Transients in HEU (4-6 mk)

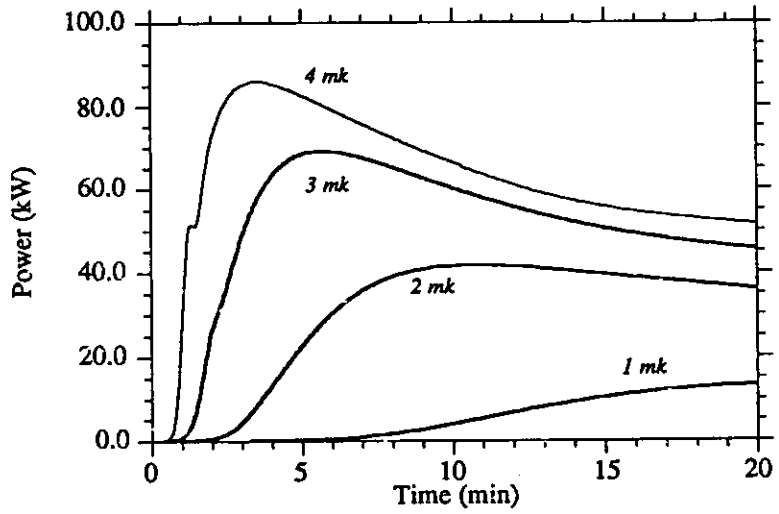

Figure 18: Self-limited Reactivity Transients in LEU (1-4 mk)

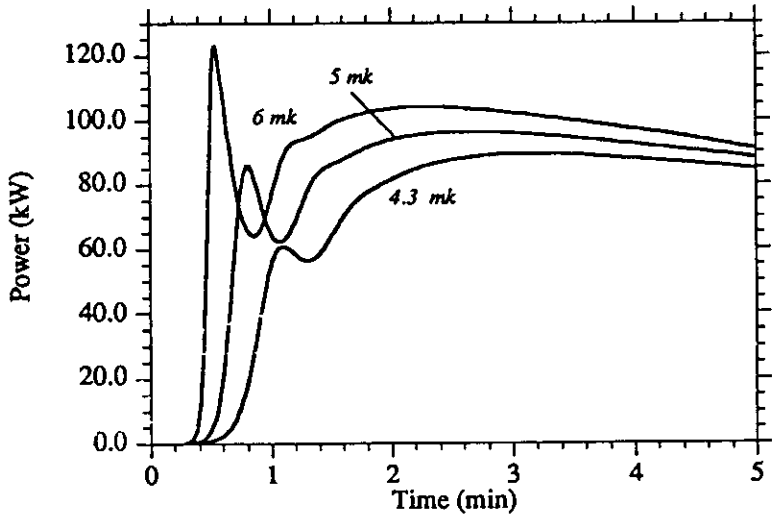

Figure 19: Self-limited Reactivity Transients in LEU (4-6 mk)

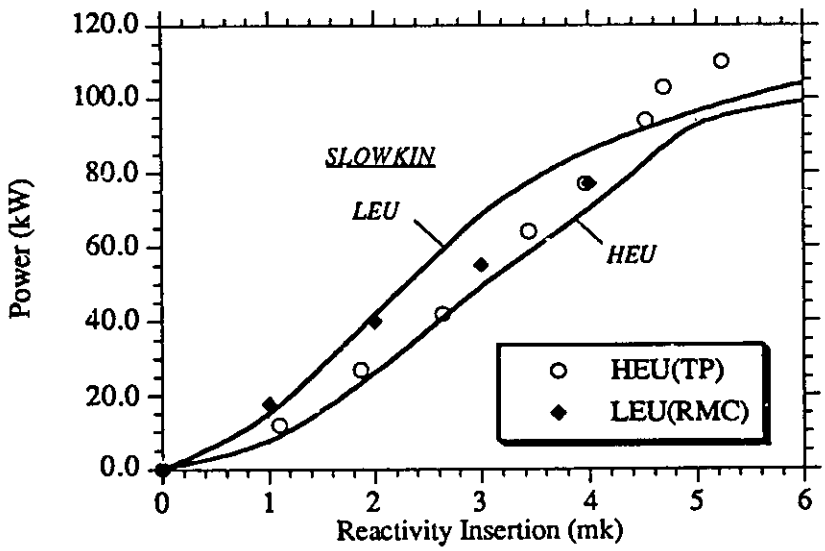

Figure 20: Delayed Peak Power in SLOWPOKE (SLOWKIN vs. measurements)

APPENDIX B

SLOWKIN INPUT FILES

B.1 Sample Input File for HEU (lump model)

```
HEU
PKIN   (FRC) (BEFF) (GEN)
       0.95   1.19   7.64E-5
COMB   HEU  (NC)   (RAC)   (H)   (DENS) (COND) (CP)
            296   .002108 0.220  3.45  0.171  0.683
GAIN   (RSI)    (RSO)   (DENS)  (COND) (CP) (HGAPO) (HCALO) (CSF)
       .002110 .002616  2.70  0.238  0.903  1.E6  0.2352 0.0045
CALP   (DENS)   (VOL)   (CP)   (RAD)  (HBE) (TAUF)
       998.2  .006931   4.182   0.11   0.2   20.
MCAL   (M) (FRAD) (PHI) (J=1,M)
       15  1.261 0.55205 0.51541 0.52828 0.54638 0.55311 0.55276
                 0.55252 0.55227 0.54591 0.52879 0.50355 0.47762
                 0.45564 0.44276 0.49610
SLAV   (NSLV) (INTERVAL) (J=1,NSLAVE+1)
       10  0.058612 0.061215 0.063818 0.066421 0.069023 0.071626
           0.074229 0.076832 0.079435 0.082037 0.084640
       (NBPINS) (J=1,NSLAVE)                          (AVGPINPOW)
           53. 76. 27. 28. 4. 46. 38. 12. 6. 5.    0.0675676
ORIF   (DINLET)  (HIN)  (DOUTLET) (HOUT)
       0.00560   0.11    0.00638   0.11
BERY   (DENS)   (VOL)   (CP)  (ROUT)  (HBE)  (LBE)
       1850.  .026519  1.499  0.21185  0.15   0.22
REFL   (DENS)   (VOL)   (CP)  (ARP)   (HRP)  (XMIX)
       998.2   .22043  4.182  1.70211  0.15   2.5
CUVE   (DENS)   (VOL)   (CP)  (ACP)   (HCP)  (TEMP)
       998.2    1.38   4.182  8.28815  0.20   20.0
PISC   (DENS)   (VOL)   (CP)  (TEMP)
       998.2   28.4477 4.182   20.0
TEMP   (PREF) 18.9 (TREF) 20.0
REAC     (A1)       (A21)       (A22)       (A3)       (A4)
       0.000917  -0.123875  -0.0015769  0.0081782  0.042226
         (A51)      (A52)
       -3.956     -4.997
BARE   (RHOB)   (Z0)   (VB)
       -0.0054  74.074   5.0
LUMP    PHOT   XENO
FIND
```